CAMBRIDGE
UNIVERSITY PRESS

Late Cambrian – Early Ordovician magmatism in the Sierra de Pie de Palo, Sierras Pampeanas (Argentina): implications for the early evolution of the proto-Andean margin of Gondwana

Carlos D. Ramacciotti[1,2] , César Casquet[3], Edgardo G. Baldo[1,2], Pablo H. Alasino[4,5], Carmen Galindo[3] and Juan A. Dahlquist[1,2]

[1]Facultad de Ciencias Exactas, Físicas y Naturales, Universidad Nacional de Córdoba, Av. Vélez Sarsfield 1611, Ciudad Universitaria, X5016CA Córdoba, Argentina; [2]Consejo Nacional de Investigaciones Científicas y Técnicas (CONICET), Centro de investigaciones en Ciencias de la Tierra (CICTERRA), Haya de la Torre s/n, Ciudad Universitaria, Córdoba, Argentina; [3]Departamento de Mineralogía y Petrología, Facultad de Ciencias Geológicas, Instituto de Geociencias (IGEO, CSIC), Universidad Complutense, 28040 Madrid, Spain; [4]Centro Regional de Investigaciones Científicas y Transferencia Tecnológica de La Rioja (Prov. de La Rioja-UNLaR-SEGEMAR-UNCa-CONICET), Entre Ríos y Mendoza s/n, Anillaco 5301, Argentina and [5]Instituto de Geología y Recursos Naturales, Centro de Investigación e Innovación Tecnológica, Universidad Nacional de La Rioja (INGeReN-CENIIT-UNLaR), Avenida Gobernador Vernet y Apostol Felipe, 5300, La Rioja, Argentina

Abstract

The Sierra de Pie de Palo, in the Argentinean Sierras Pampeanas (Andean foreland), consists of a Mesoproterozoic basement and an Ediacaran – upper Cambrian sedimentary cover that underwent folding, thrusting and metamorphism during the Ordovician Famatinian orogeny. Mafic rocks and granitoids of the easternmost Sierra de Pie de Palo provide information about the magmatic activity at the proto-Andean margin of Gondwana during late Cambrian – Early Ordovician time. Magmatic activity began in the Sierra de Pie de Palo as dykes, sills and small intrusions of tholeiitic gabbros between 490 and 470 Ma, before shortening and regional metamorphism. Variable mantle sources (Nd depleted mantle age, T_{DM} between 1.7 and 1.3 Ga) were involved in the mafic magmatism. Nd-isotope signatures were probably inherited from a Mesoproterozoic subcontinental mantle. Mafic magmatism was coincident with collapse of a Cambrian carbonate-siliciclastic platform that extended along SW Gondwana, and was probably coeval with the beginning of subduction. After mafic magmatism, peraluminous granitoids were emplaced in the Sierra de Pie de Palo along ductile shear zones during a contractional tectonic phase, coeval with moderate to high P/T metamorphism, and with the Cordilleran-type magmatic arc that resulted from a flare-up at *c.* 470 Ma. Granitoids resulted mainly from partial melting of metasedimentary rocks, although some hybridization with juvenile magmas and/or rocks cannot be ruled out. The evidence shown here further implies that the Pie de Palo block was part of the continental upper plate during the Famatinian subduction, and not an exotic block that collided with the Gondwana margin.

1. Introduction

Active continental margins are complex regions consisting of a variety of morphotectonic domains such as accretionary wedges, marginal basins and highs, and magmatic arcs (Kopp, 2013). Tectonic erosion of the upper plate and subduction of oceanic plateaus can suppress one or more of the morphotectonic domains and lead to segmentation of the margin, adding complexity to the overall structure (e.g. Malavieille & Trullenque, 2009). Active continental margins may further involve accretion of foreign oceanic or continental ribbons, a common process throughout the Earth history (Cawood *et al.* 2009).

Recognizing the structure and dynamics of active continental margins in the case of fossil margins is often difficult if they were the locus of a protracted orogenic history. In this contribution we examine the history of the proto-Andean margin of Gondwana in the Sierras Pampeanas of Argentina, which turned active during late Cambrian – Early Ordovician time starting the Famatinian orogeny (e.g. Pankhurst *et al.* 1998; Sims *et al.* 1998; Steenken *et al.* 2006; Dahlquist *et al.* 2008, 2013; Rapela *et al.* 2018). The term Famatinian Cycle was proposed by Aceñolaza & Toselli (1973) to refer to a period of deformation, magmatism, metamorphism and sedimentation between late Cambrian and Middle Devonian time. However, later studies demonstrated that the main tectonic activity occurred between late Cambrian and Middle Ordovician time (e.g. Pankhurst *et al.* 1998; Ramos *et al.* 1998). The Famatinian belt extends between Patagonia and Venezuela along the continent margin (see review in Ramos, 2018)

and was part of the long Terra Australis orogen (*c.* 18 000 km) defined by Cawood (2005) that fringed SW Gondwana during the early Palaeozoic Era. The width of this orogenic belt in the Sierras Pampeanas of Argentina is *c.* 500 km and it preserves excellent vertical sections (from roof to top of the magmatic arc), providing a unique opportunity to study this orogen (Fig. 1a). Evidence of deformation, metamorphism and magmatism between *c.* 490 and 440 Ma has long been recognized in the easternmost Sierras Pampeanas, in the Puna (Altiplano) of northern Argentina and in Patagonia, as well as in Chile (e.g. Bahlburg & Hervé, 1997; Rapela *et al.* 1998; Pankhurst *et al.* 2000, 2014, 2016; Büttner *et al.* 2005; Dahlquist *et al.* 2008; Drobe *et al.* 2011; Steenken *et al.* 2011; Mulcahy *et al.* 2014).

The tectonic evolution of the Famatinian belt is still poorly understood. Several longitudinal (N–S) domains have been recognized on the basis of stratigraphic records, types of magmatism and radiometric ages (e.g. Bahlburg & Hervé, 1997; Grosse *et al.* 2011; Rapela *et al.* 2018), but their geodynamic significance is not yet well established. One of these such domains is unanimously considered a Cordilleran-type magmatic arc with I-type magmatism (gabbro to monzogranite), and crops out in the central part of the belt (Fig. 1a; e.g. Grosse *et al.* 2011). Based on this magmatic arc, the Famatinian belt was conventionally interpreted as an orogen resulting from subduction along the continental margin (e.g. Bahlburg & Hervé, 1997; Astini & Dávila, 2004; Coira *et al.* 2009). Some authors (e.g. Ramos, 1988; Astini *et al.* 1995; Astini & Dávila, 2004) have further related the early evolution of the Famatinian orogeny to the Ordovician collision of the allegedly exotic Laurentia-derived Precordillera/Cuyania terrane with the proto-Andean margin of Gondwana. This terrane is named after the Argentine Precordillera, which is located west of the Sierras Pampeanas in western Argentina (Fig. 1a) (for a review of this terrane and its extension into the Sierras Pampeanas, see Ramos, 2004). However, there is no consensus regarding the boundaries and time accretion of this terrane (see discussion section of this paper; Finney, 2007).

This work focuses on the Sierra de Pie de Palo in the western Sierras Pampeanas of Argentina belonging to the western domain of the Famatinian orogeny (Rapela *et al.* 2018), to the west of the Cordilleran-type magmatic arc, which is well exposed in the Famatina and Valle Fértil ranges (Fig. 1). We present new whole-rock elemental chemistry, Sr- and Nd-isotopes, and geochronological (U–Pb SHRIMP zircon ages) data from granitoids and mafic rocks of the Sierra de Pie de Palo in order to assess the probable source of magmas and the tectonic significance of this magmatism. We also discuss the palaeogeographic implication of these igneous rocks for the early Palaeozoic evolution of the proto-Andean margin of Gondwana.

2. Geological setting

The Sierra de Pie de Palo is one of the westernmost ranges of the Sierras Pampeanas of Argentina (Fig. 1a) which resulted from the tilting and uplift of foreland blocks during the Cenozoic Andean orogeny (e.g. Jordan & Allmendinger, 1986). The Sierra de Pie de Palo is a young (Andean) dome resulting from gentle folding of the pre-Andean basement. The basement consists of an E-dipping syn-metamorphic ductile thrust stack produced during the Famatinian orogeny with a dominantly top-to-the-W sense of movement (e.g. Casquet *et al.* 2001; Mulcahy *et al.* 2011). Structural depth increases westwards towards the Pirquitas thrust

(Fig. 1b) at the bottom of the pile. This basal thrust has a complex tectonic history (Ramos *et al.* 1998; van Staal *et al.* 2011). The tectonic nappes consist of a reworked Mesoproterozoic basement and a Neoproterozoic – upper Cambrian sedimentary cover that underwent tight recumbent folding (F1) and development of a penetrative syn-metamorphic foliation (S1; Fig. 2), almost coeval with underthrusting at ≥ 460 Ma (Casquet *et al.* 2001). A younger fold phase (F2), which shows steep axial planes, is recognized in the southern Sierra de Pie de Palo. Extensional shear zones – apparently older than F2 – were described in the east (Casquet *et al.* 2001) such as the Nikizanga Shear Zone, which has yielded a muscovite $^{40}Ar/^{39}Ar$ age of *c.* 440 Ma (Mulcahy *et al.* 2011). Cenozoic reverse faults further reworked the Palaeozoic assembly and are well exposed in the easternmost slope of the range (Fig. 2) (Bellahsen *et al.* 2016). Ordovician metamorphism in Ca-pelitic schist of the central part of the Sierra de Pie de Palo reached upper low- to medium-grade conditions (*c.* 1.3 GPa and 600°C) under a moderate to high P/T metamorphism, coeval with folding and thrusting (Baldo *et al.* 1998; Casquet *et al.* 2001).

From west to east, the Sierra de Pie de Palo is mainly composed of the following lithostratigraphic units: Caucete Group, Pie de Palo Complex, Central Complex, Difunta Correa Metasedimentary Sequence and Nikizanga Group. The Mesoproterozoic basement comprises a Grenvillian (*sensu lato*) ophiolite complex in the west and a poorly known meta-igneous and metasedimentary complex in the central and western part of the range (Fig. 1b). Both were variably reworked by the Famatinian orogeny. The ophiolite units constitute the Pie de Palo Complex, exposed between the Pirquitas and Duraznos thrusts. It consists mainly of mafic and ultramafic rocks, with minor outcrops of felsic rocks (tonalite–trondhjemite–granodiorite) (Pankhurst & Rapela, 1998; Vujovich & Kay, 1998). The age of the igneous rocks of the complex ranges between *c.* 1030 Ma and *c.* 1245 Ma (Vujovich *et al.* 2004; Morata *et al.* 2010; Rapela *et al.* 2010; Mulcahy *et al.* 2011). The Central Complex, between the Duraznos and Morales ductile thrusts, consists of schists, quartzites, marbles, metavolcanic rocks, migmatites, orthogneisses and amphibolites (Casquet *et al.* 2001; Mulcahy *et al.* 2011). One orthogneiss yielded an protolith age of *c.* 1280 Ma (Garber *et al.* 2014), while an anorogenic A-type orthogneiss yielded an protolith age of *c.* 774 Ma and was attributed to the early break-up of the Rodinia supercontinent (Baldo *et al.* 2006). The ages of Garber *et al.* (2014) imply that the depositional age of metasedimentary rocks of the Central Complex was Mesoproterozoic or older.

The Neoproterozoic Difunta Correa Metasedimentary Sequence, first recognized by Baldo *et al.* (1998), is best exposed in the central and eastern parts of the range (Fig. 1b). This sequence consists of medium-grade metamorphic rocks from four lithostratigraphic units (Ramacciotti *et al.* 2015*b*), consisting of metasiliciclastic rocks (metaconglomerate to metapelite) and thick marbles. Sedimentation was dated as Ediacaran (*c.* 620 Ma) on the basis of the Sr-isotope composition of marbles and U–Pb detrital zircon ages (Galindo *et al.* 2004; Rapela *et al.* 2005; Ramacciotti *et al.* 2015*a*).

The Cambrian section of the sedimentary cover is represented by the Caucete and Nikizanga groups. The Caucete Group (Borello, 1969) crops out in the western slope of the range, at the footwall of the Pirquitas thrust (Fig. 1b). It is mainly composed of low- to medium-grade metamorphic rocks, such as metasandstones and marbles, and to a lesser extent metavolcaniclastic rocks. The Nikizanga Group, in the southeastern slope of the range (Fig. 2),
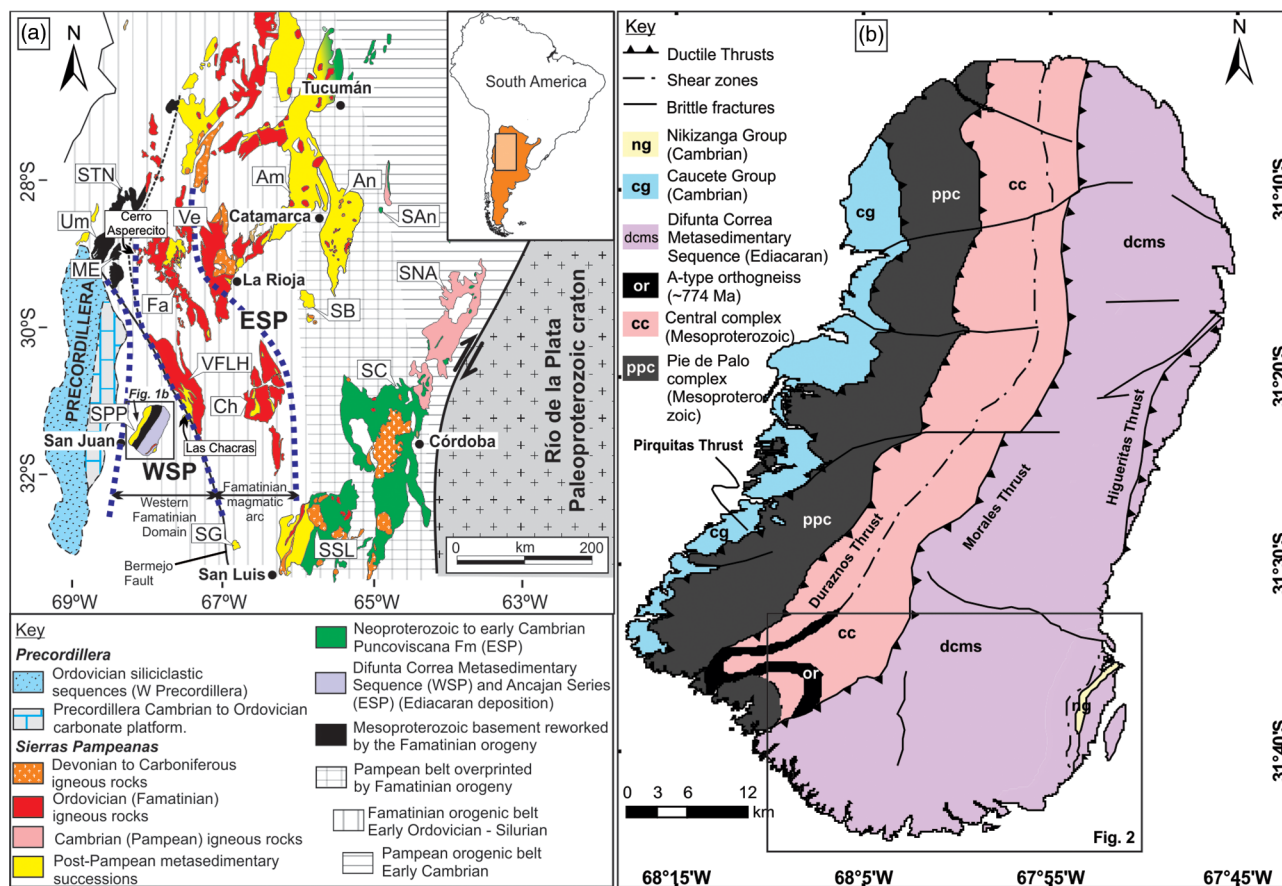
Fig. 1. (Colour online) (a) Schematic geological map of the Sierras Pampeanas and the Precordillera (modified from Rapela *et al.* 2016). Am – Sierra de Ambato; An – Sierra de Ancasti; CA – Cerro Asperecito; Ch – Sierra de Chepes; Fa – Sierra de Famatina; ME – Sierra de Maz and Espinal; LC – Las Chacras; SAn – Sierra de Ancaján; SB – Sierra Brava; SC – Sierras de Córdoba; SG – Sierra del Gigante; SNA – Sierra Norte-Ambargasta; WSP – western Sierras Pampeanas; ESP – eastern Sierras Pampeanas; SPP – Sierra de Pie de Palo; SSL – Sierra de San Luis; STN – Sierra del Toro Negro; UM – Sierra de Umango; Ve – Sierra de Velasco; VFLH – Sierra de Valle Fértil-La Huerta. (b) Simplified geological map of the Sierra de Pie de Palo showing the main lithological units and structures (modified after Ramos & Vujovich, 2000; Casquet *et al.* 2001; Mulcahy *et al.* 2011; Ramacciotti *et al.* 2015a).

consists of low- to medium-grade metamorphic rocks such as graphitic schist, phyllite, quartzite and marble (CD Ramacciotti, PhD thesis, Universidad Nacional de Córdoba, 2016). Both groups (Caucete and Nikizanga) were deposited between 525 and 490 Ma in a mixed carbonate-siliciclastic platform, fringing the SW Gondwana margin that extended at least from Patagonia to northwestern Argentina (Ramacciotti *et al.* 2018).

Mafic meta-igneous bodies (transposed sills and small stocks hosted mainly in metasedimentary rocks; this work) older than the Famatinian F1 folding, thrusting and regional metamorphism and syn-metamorphic peraluminous granitoids have long been recognized in the eastern slope of the Sierra de Pie de Palo (Fig. 2; Pankhurst & Rapela, 1998; Mulcahy *et al.* 2011; Baldo *et al.* 2012; this work). Their tectonic significance is reviewed in this contribution along with new geochemical and geochronological data.

3. Mafic rocks and granitoids of the Sierra de Pie de Palo

Although some Ordovician felsic rocks were described by some authors in the Sierra de Pie de Palo (Mulcahy *et al.* 2011; Baldo *et al.* 2012), the mafic units of this age remained poorly known before this contribution. These mafic igneous bodies were overprinted by regional metamorphism and shearing, whereas the felsic units, with the exception of the La Chilca Granite, were variably

affected by ductile shearing only. F1 folding of mafic rocks is recognized (Fig. 2). Mafic rocks are found in the upper nappe of the thrust stack to the east of the El Indio ductile thrust zone. They are metagabbros, metagabbrodiorites or amphibolites, depending on whether they show a metamorphic foliation or preserve the primary texture. Mafic bodies were originally dykes, sills or small intrusions that were transposed and converted through deformation into elongated bodies of up to 3000 m long and 200 m thick (Figs 2, 3a). They intruded the Difunta Correa Metasedimentary Sequence and the Nikizanga Group, and were themselves intruded by felsic magmas, implying that mafic rocks are older than the granitoids. The mafic rocks are coarse- to fine-grained (1 cm to 0.1 mm; Fig. 3), the metagabbros and metagabbrodiorites show inherited granular igneous texture (Figs 3b, c), and the amphibolites show nematoblastic texture with foliation defined by amphibole orientation (Fig. 3d, e). Primary minerals were converted in all mafic rocks into a secondary low- to medium-grade metamorphic assemblage of Amph (tremolite and Mg-hornblende), with lesser amounts of Bt, Pl, Qz, Ttn, Zrn and Ilm (mineral abbreviations after Whitney & Evans, 2010).

Granitoids are mainly found within the El Indio ductile thrust zone, except for one small pluton (La Chilca Granite). The El Indio ductile thrust zone is a steep E-dipping NE–SW shear zone with a reverse top-to-the-W sense of motion (Fig. 4a, b), and probably
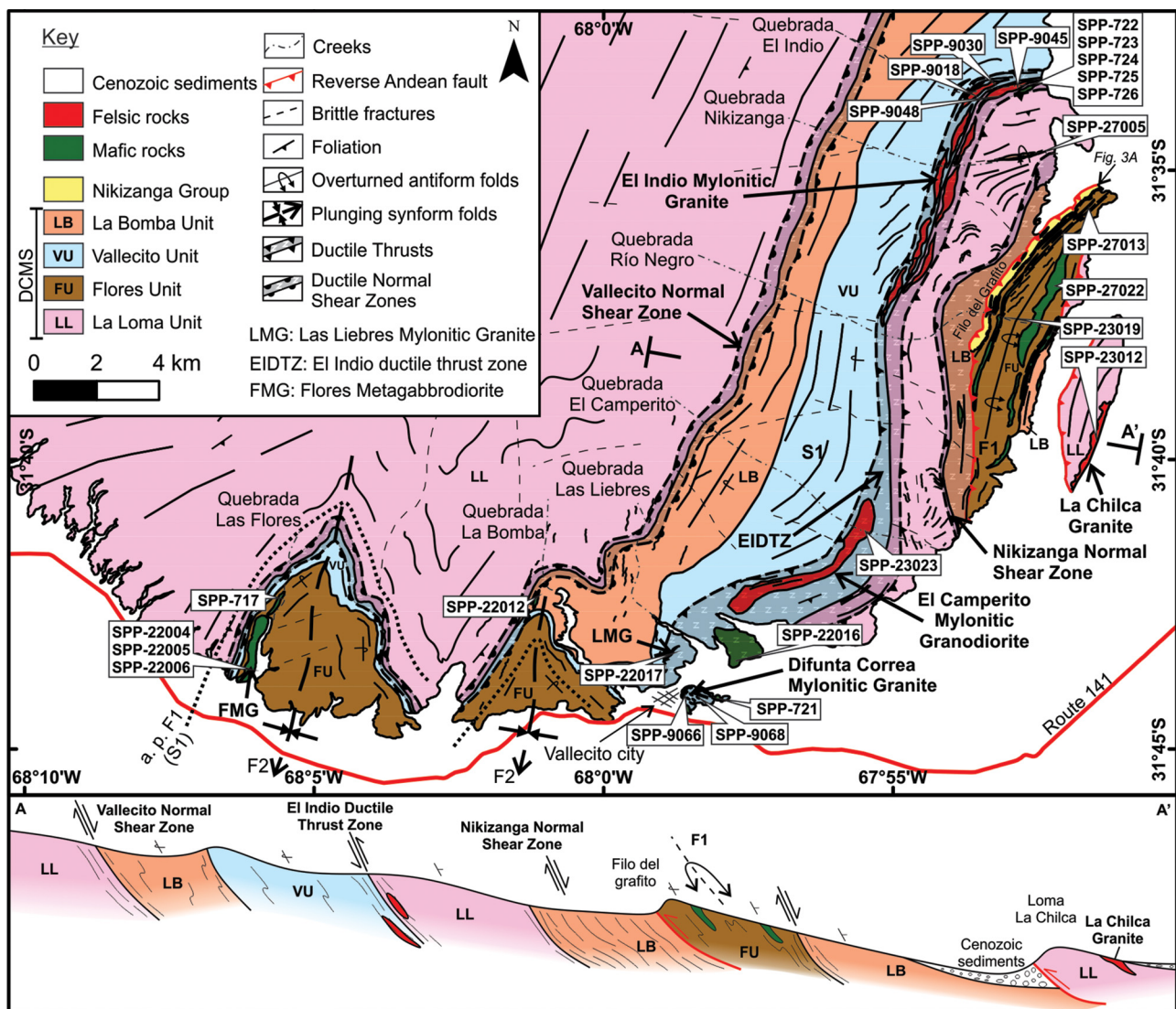
Fig. 2. (Colour online) Geological map (upper) of southeastern Sierra de Pie de Palo showing the location of mafic rocks and granitoids studied here, and schematic geologicalal cross-section (lower). a.p. – axial planar foliation; DCMS – Difunta Correa Metasedimentary Sequence.

represents the southern extension of the Higueritas shear zone described by Mulcahy *et al.* (2011). The host rocks of the granitoids are sheared metasedimentary rocks of the Difunta Correa Metasedimentary Sequence and, locally, the mafic igneous rocks described above. Several granitoids are discussed here, described in the following.

The El Indio Mylonitic Granite consists of sheets of granodiorites to (mainly) granites with a general NE–SW orientation. This unit was described by Baldo *et al.* (2012) as consisting mainly of porphyritic to equigranular biotite-garnet monzogranite and aplite. The mineral assemblage is $Qz - Kfs - Pl_{(An\ 20-28)} - Ep_{(Czo)} - Bt_{(Al}^{iv}$ $_{2.6,\ XFe\ 0.7,\ Ti\ 0.3)} - Grt_{(Alm\ 70.1,\ Sps\ 21.5,\ Py\ 5.5,\ Grs\ 1.9)} - Ms - Zrn - Ap - Opq$. K-feldspar and garnet form porphyroclasts (*c.* 4 mm) in a mylonitic flow texture with abundant ribbon quartz.

The Difunta Correa Mylonitic Granite is a small lens-shaped intrusion near Vallecito town. It was affected by the southern extension of the El Indio ductile thrust zone and was described by Baldo *et al.* (2012) as a medium-grained leucocratic granite composed of $Qz - Kfs_{(Or90.5)} - Pl_{(An16.2\ to\ An21)} - Ms_{(Si\ 6.13,\ Al}^{iv}$ $_{1.87,\ XFe\ 0.6)} - Bt_{(Al}^{iv}\ _{2.5,\ XFe\ 0.69,\ Ti\ 0.3)} - Grt_{(Alm\ 65.2,\ Sps\ 25.6,\ Py\ 5.5,}$

$_{Grs\ 3.5)} - Zrn - Ap_{(F\ \sim\ 3\%)}$. It has a mylonitic texture defined by porphyroclasts of garnet and K-feldspar (*c.* 3 mm), aligned micas and several subgrained minerals. Garnet compositions in both the El Indio and Difunta Correa mylonitic granitoids are typical of igneous origin (Dahlquist *et al.* 2007; Baldo *et al.* 2012).

The Las Liebres Mylonitic Granite corresponds to a small transposed dyke (< 2 m thick) within the El Indio ductile thrust zone (Fig. 4c). Its mineral association is $Qz - Kfs - Pl - Ms - Grt - Ep - Zrn - Opq$. K-feldspar and garnet porphyroclasts (*c.* 5 mm) are surrounded by a fine-grained matrix mainly composed of quartz, plagioclase, epidote and muscovite (Fig. 4d).

The El Camperito Mylonitic Granodiorite forms a NE–SW elongated pluton *c.* 4 km long and 200 m wide, which intruded the marbles of the Difunta Correa Metasedimentary Sequence (Fig. 4e). It has the mineral assemblage $Qz - Kfs - Pl - Bt - Ep - Ap - Zrn - Aln - Opq$. The mylonitic texture is formed by *c.* 5 mm K-feldspar porphyroclasts, set in a fine-grained matrix mainly composed of quartz, plagioclase and biotite (Fig. 4f).

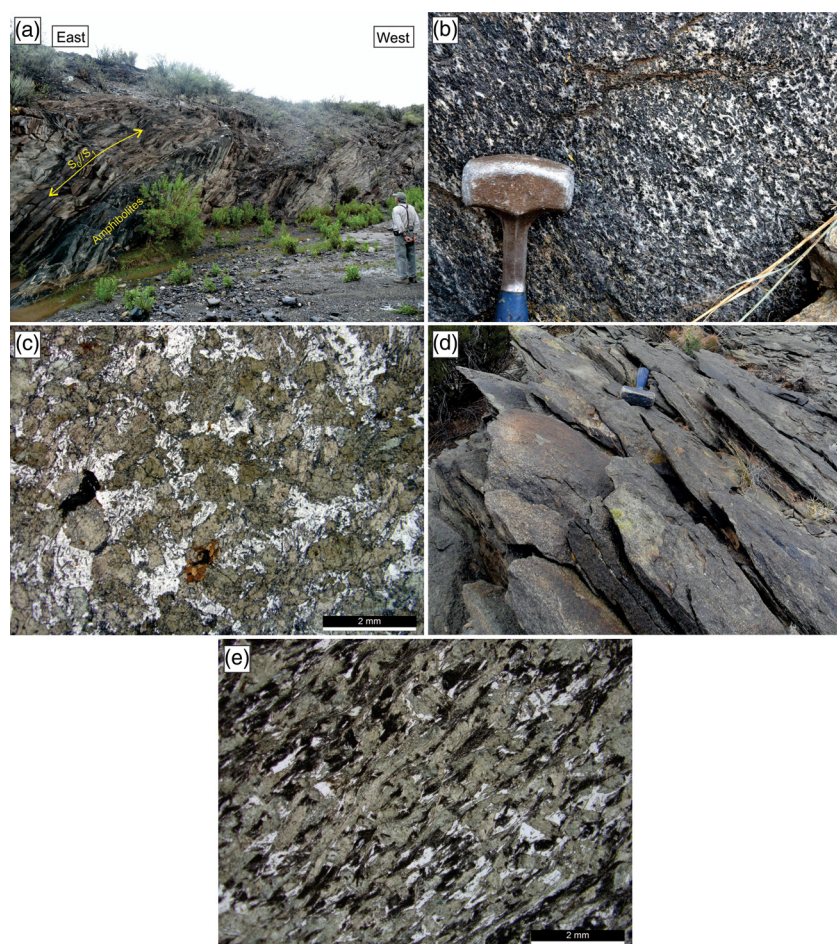The La Chilca Granite is an elongated body (2 km long and 100 m wide) outside the El Indio ductile thrust zone.

Fig. 3. (Colour online) Mafic rocks of southeastern Sierra de Pie de Palo. (a) Amphibolite lens wrapped by the foliation S1 that is parallel to S0 in the flank of an overturned fold in the Nikizanga Group (location in map, Fig. 2). (b) Weakly foliated metagabbro (the primary igneous texture can be still recognized). (c) Plane-polarized light (PPL) photomicrograph of non-foliated metagabbro, showing the primary granular texture composed of Amph – Pl – Qz – Bt – Ttn – Ilm. (d) Amphibolites in outcrop. (e) Photomicrograph (PPL) of one amphibolite showing metamorphic penetrative foliation.

It discordantly cuts the hosting quartz schists (Difunta Correa Metasedimentary Sequence) and is covered by Tertiary sediments on the eastern side (Figs 2, 4g, h). The mineral assemblage of this granite is Qz – Kfs – Pl – Ms – Bt – Grt – Ep – Zrn – Opq and it is fine- to medium-grained (< 5 mm) (Fig. 4h). It is locally deformed by ductile shear zones. The age of this granite is unknown and it will not be discussed further here.

4. Sampling and analytical methods

Chemical analyses (major, minor and trace elements) and isotope determinations (Rb–Sr and Sm–Nd) were carried out on 25 samples of mafic rocks and granitoids from the southeastern Sierra de Pie de Palo. Sample numbers along with their location and rock names are given in Table 1.

Eighteen samples were analysed at Activation Laboratories Ltd (Actlabs, Ontario, Canada) following the 4E-Litho-research routine. Major elements were determined by inductively coupled plasma (ICP) atomic emission spectroscopy (AES), whereas minor and trace elements were determined by ICP mass spectrometry (MS). The remaining six samples were analysed by X-ray fluorescence (XRF) at the Laboratory of the Instituto de Geología y Minería, Universidad Nacional de Jujuy, Argentina, on a Rigaku FX2000 spectrometer with Rh tube. Ground and homogenized samples were fused with lithium tetraborate for major-element analyses. Results are given in online Supplementary Table S1 (available at http://journals.cambridge.org/geo) along with detection limits and standard measurement.

Rb–Sr and Sm–Nd isotope analyses were carried out on 13 samples (online Supplementary Table S2). Seven analyses from this group were mentioned but not published by Baldo *et al.* (2012). Concentrations of Rb and Sr, as well as Rb/Sr atomic ratios, were determined by XRF spectrometry at the X-Ray Diffraction Center of the Complutense University, following the methods of Pankhurst & O'Nions (1973). Isotope analysis was carried out at the Geochronology and Isotope Geochemistry Center of the Complutense University of Madrid on a Phoenix automated multicollector mass spectrometer (sixsamples) and on an automated multicollector VG Sector 54 mass spectrometer (seven samples). Analytical procedures are described in Casquet *et al.* (2010). Replicate analyses of the NBS-987 Sr-isotope standard yielded an average $^{87}Sr/^{86}Sr$ ratio of 0.71024 ± 0.00003 (2σ) and 0.71027 ± 0.00004 (2σ) respectively; accepted value, 0.71025 ± 0.00002 (Faure, 2001).

Sm and Nd were determined by isotope dilution using spikes enriched with ^{149}Sm and ^{150}Nd and were separated from other rare Earth elements (REE) using bio-beads coated with 10% diethylhexyl phosphoric acid. Quoted errors are two standard deviations (2σ); the decay constant λ ^{147}Sm was taken as 6.54 × 10^{-12} a^{-1} (Lugmair & Marti, 1978). Analytical uncertainties are estimated to be 0.006% for $^{143}Nd/^{144}Nd$ and 0.1% for $^{147}Sm/^{144}Nd$ ratios. Eight analyses of La Jolla Nd-standard were measured during sample analysis, and gave a mean $^{143}Nd/^{144}Nd$ ratio of 0.511845 ± 0.000001 (2σ) (Phoenix) and 0.511854 ± 0.000004 (2 s) (VG Sector 54); accepted value, 0.511859 ± 0.000007 (Lugmair & Carlson, 1978).
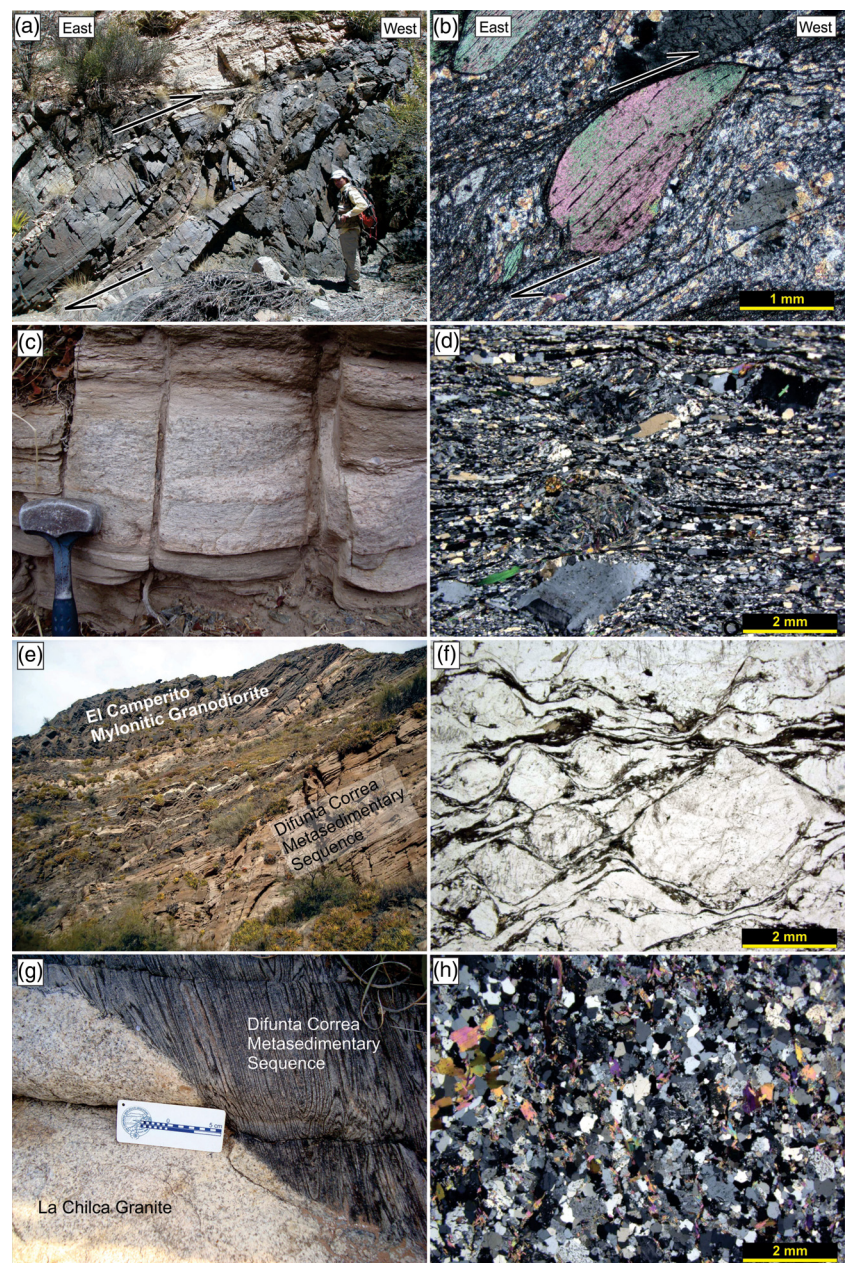
Fig. 4. (Colour online) Granitoids of the Sierra de Pie de Palo. (a) El Indio ductile thrust zone showing top-to-the-W sense of motion. Dark rocks correspond to metamorphic units of the Difunta Correa Metasedimentary Sequence. (b) Photomicrograph of mica-fish in the El Indio Ductile Thrust, showing sense of movement. (c) The Las Liebres Mylonitic Granite (LMG). (d) Cross-polarized light (XPL) photomicrograph of the LMG, showing the mylonitic texture with quartz ribbons and subgrained feldspar porphyroclasts. (e) The El Camperito Mylonitic Granodiorite (ECMG) hosted by marbles of the Vallecito Unit (Difunta Correa Metasedimentary Sequence). (f) Photomicrograph (PPL) showing the mylonitic texture of the ECMG. (g) The La Chilca Granite (LCG) hosted by quartz-schists of the La Loma Unit (Difunta Correa Metasedimentary Sequence). (h) Photomicrograph (XPL) of the LCG showing the hypidiomorphic, inequigranular texture.

One metagabbrodiorite from Quebrada Las Flores (SPP-22004) and two samples of granitoids (SPP-22017, a mylonitic granite from the Las Liebres Mylonitic Granite; SPP-23023, a mylonitic granodiorite from the El Camperito Mylonitic Granodiorite) were collected for U–Pb SHRIMP zircon dating. Zircons were separated and concentrated using standard crushing, washing, heavy liquids and paramagnetic separation procedures as described by Rapela *et al.* (2007). The zircon-rich heavy mineral concentrates were poured onto double-sided tape, mounted in epoxy together with chips of the Temora reference zircon, sectioned approximately in half, and polished. Cathodoluminescence images were used to describe the internal structures of the sectioned grains. Samples were analysed with SHRIMP RG, following the methods proposed by Williams (1998), at the Research School of Earth Sciences, The Australian National University (Canberra, Australia). Each analysis consisted of four scans through the mass range, and the reference zircon was analysed once every five unknowns. Data were reduced using Isoplot/Ex (Ludwig, 2003) and are given in online Supplementary Table S3 (available at http://journals.cambridge-e.org/geo). Common Pb corrections for ages older than 800 Ma were made using ^{204}Pb and for younger ages by means of ^{207}Pb (Williams, 1998). Analyses with high common Pb (> 5%), discordance > 10% and error age (1σ) > 5% were discarded and not considered in the probability density plots.

5. Whole-rock geochemistry

5.a. Elemental chemistry

5.a.1. Mafic rocks

Geochemical data from 12 samples of mafic rocks from the Sierra de Pie de Palo are shown in online Supplementary Table S1. Metagabbros and metagabbrodiorites ($n = 9$) are chemically similar to amphibolites ($n = 3$) except for the loss on ignition content

Table 1. Location, rock-type and type of analytical determinations carried out on mafic rocks and granitoids from the southeastern Sierra de Pie de Palo. LMG – Las Liebres Mylonitic Granite; LCG – La Chilca Granite; ECMG – El Camperito Mylonitic Granodiorite; EIMG – El Indio Mylonitic Granite; DCMG – Difunta Correa Mylonitic Granite.

Sample number	Latitude (S)	Longitude (W)	Unit	Location
SPP-22004	31° 43′ 44′′	68° 06′ 05′′	Metagabbrodiorite	Quebrada Las Flores
SPP-22005	31° 43′ 44′′	68° 06′ 07′′	Metagabbrodiorite	Quebrada Las Flores
SPP-22006	31° 43′ 47′′	68° 06′ 09′′	Metagabbro	Quebrada Las Flores
SPP-23019	31° 41′ 04′′	67° 55′ 14′′	Metagabbro	Quebrada Río Negro
SPP-27005	31° 34′ 44′′	67° 52′ 35′′	Metagabbrodiorite	Quebrada Nikizanga
SPP-27013	31° 35′ 44′′	67° 51′ 43′′	Metagabbro	North Filo del Grafito
SPP-27022	31° 37′ 28′′	68° 07′ 52′′	Metagabbro	East Filo del Grafito
SPP-717	31° 42′ 22′′	68° 05′ 43′′	Metagabbro	Quebrada Las Flores
SPP-721	31° 44′ 21′′	67° 58′ 02′′	Metagabbro	Difunta Correa
SPP-22012	31° 42′ 25′′	68° 01′ 10′′	Amphibolite	Quebrada La Bomba
SPP-22016	31° 43′ 31′′	67° 57′ 42′′	Amphibolite	Quebrada Las Liebres
SPP-722	31° 33′ 32′′	67° 52′ 19′′	Amphibolite	Quebrada El Indio
SPP-22017	31° 43′ 17′′	68° 00′ 40′′	LMG	Quebrada Las Liebres
SPP-23012	31° 40′ 17′′	67° 51′ 46′′	LCG	Loma La Chilca
SPP-23023	31° 40′ 57′′	67° 55′ 21′′	ECMG	Quebrada El Camperito
SPP-723	31° 33′ 32′′	67° 52′ 19′′	EIMG	Quebrada El Indio
SPP-724	31° 33′ 32′′	67° 52′ 19′′	EIMG	Quebrada El Indio
SPP-725	31° 33′ 32′′	67° 52′ 19′′	EIMG	Quebrada El Indio
SPP-726	31° 33′ 32′′	67° 52′ 19′′	EIMG	Quebrada El Indio
SPP-9018	31° 33′ 34′′	67° 54′ 01′′	EIMG	Quebrada El Indio
SPP-9030	31° 33′ 34′′	67° 53′ 29′′	EIMG	Quebrada El Indio
SPP-9045	31° 33′ 30′′	67° 52′ 54′′	EIMG	Quebrada El Indio
SPP-9048	31° 33′ 47′′	67° 52′ 43′′	EIMG	Quebrada El Indio
SPP-9066	31° 43′ 58′′	67° 58′ 34′′	DCMG	Vallecito City
SPP-9068	31° 44′ 04′′	67° 58′ 29′′	DCMG	Vallecito City

(0.26–1.16% in the former and 1.02–2.42% in the latter), so they will be described together: $SiO_2 = 47.9$–53.3%; $Na_2O + K_2O = 1.8$–2.9%; $FeO^t + MgO = 14.8$–17.8%; and Mg no. $(100 \times MgO/(MgO+FeO^t)$ molar) = 49.9–71.3. In the Winchester & Floyd (1977) classification scheme, based on the ratios of immobile elements Zr/TiO_2 versus Nb/Y (Fig. 5a), the mafic rocks cluster in the andesite/basalt field, suggesting only minor chemical modification after deformation and metamorphism. The mafic rocks are metaluminous with alumina saturation index (ASI) values of 0.55–0.65 and correspond to the tholeiitic series, as shown in the TiO_2 versus FeO^t/MgO diagram of Miyashiro (1974) (Fig. 5b). This interpretation is strengthened in a normalized mid-ocean-ridge basalt (N-MORB) immobile element plot (Fig. 5c), where the mafic rocks exhibit a typical tholeiitic pattern (Pearce, 1996). The concentration of Cs is between 0.2 and 0.7 ppm, Rb = 10–20 ppm, Ba = 82–147 ppm, Sr = 120–152 ppm, and the high-field-strength elements (HFSEs) show values of Nb < 3.6, Ta < 0.8 and Zr < 95 ppm. In the Nb–Zr–Y diagram of Meschede (1986) the mafic rocks plot in the field of N-MORB and arc basalts (Fig. 5d). REE contents normalized to chondrite (Sun & McDonough, 1989) exhibit flat patterns ($La_N/Yb_N = 1.9$–2.6), with

slightly negative Eu anomalies (Eu/Eu* = 0.80–0.87) (Fig. 5e). The multi-element plot normalized to N-MORB (Sun & McDonough, 1989) shows a slight enrichment in light REEs but high values of Cs, Rb, Ba, Th, U and K (Fig. 5f). The concentration of Sr, Nd, Nd, Zr and middle/heavy REEs are slightly low or similar to N-MORB. Remarkably, in spite of the conversion of mafic rocks to low- to medium-grade metamorphic mineral assemblages, they have largely preserved the original chemical composition with the exception of H_2O.

5.a.2. Granitoids

Geochemical data from 12 granitoids are shown in online Supplementary Table S1. They exhibit variable contents of SiO_2 (65.5–76.4%), $Na_2O + K_2O$ (7.4–11.6%) and CaO (0.7–3.1%). The CaO/Na_2O ratios range from 0.23 to 0.88, and the Al_2O_3/TiO_2 ratios from 39 to 242, except for one sample that shows a value of 1401. Nine of those samples have SiO_2 contents of 71.6–76.4% (i.e. granites according to the TAS plot; not shown), one sample (SPP-723) is from a K-feldspar-rich facies, and the other two (SPP-9030 and SPP-23023) are mylonitic granodiorites with SiO_2 content of *c.* 66%. All these rocks are slightly or moderately peraluminous
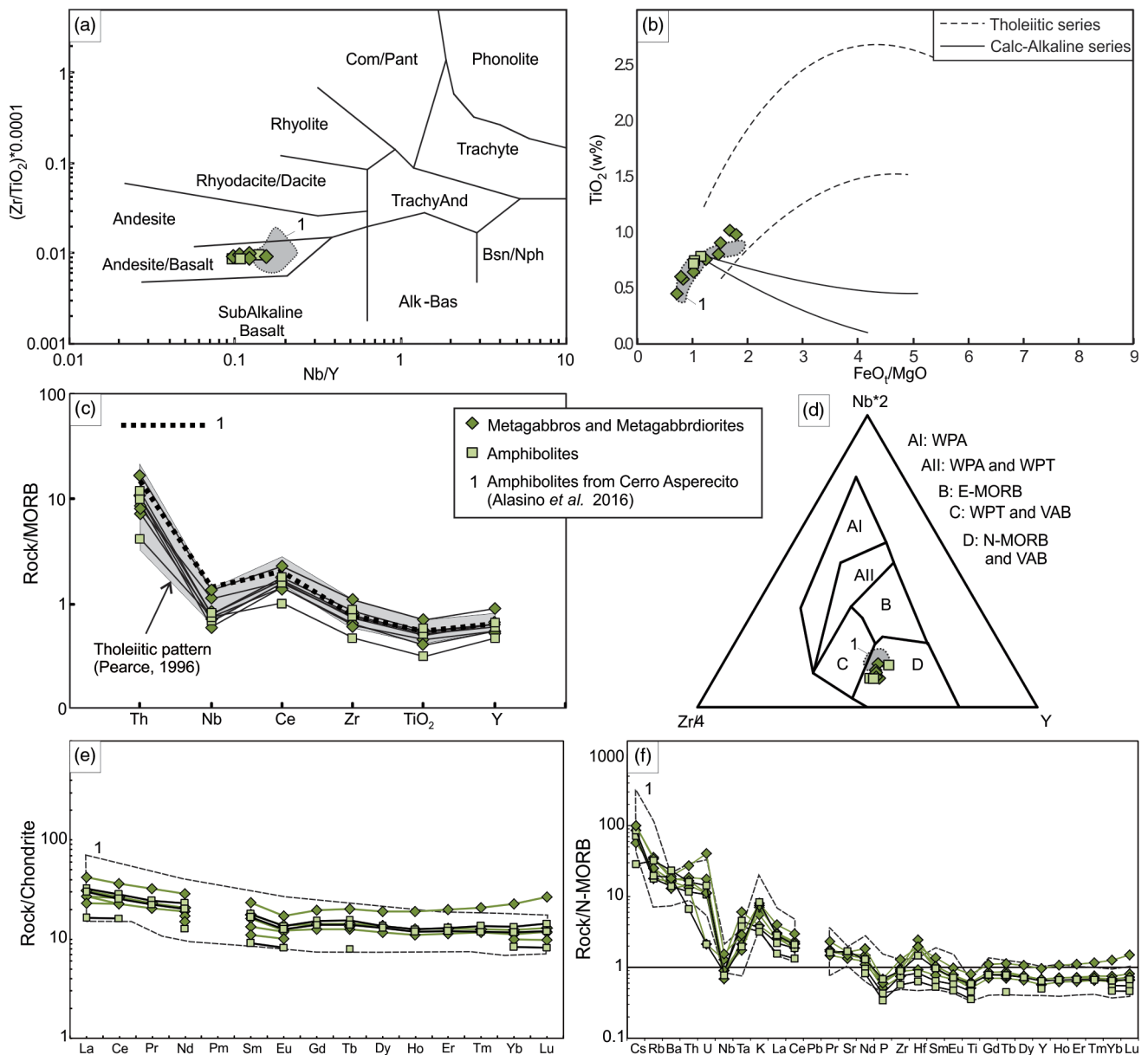
Fig. 5. (Colour online) Geochemical diagrams of mafic rocks from the Sierra de Pie de Palo and equivalents from elsewhere. (a) Winchester & Floyd (1977) classification of volcanic rocks. (b) Diagram to discriminate between tholeiitic and calc-alkaline series, after Miyashiro (1974). (c) Rock/MORB multi-element plot of mafic rocks from Sierra de Pie de Palo and the field of tholeiites (shaded area) (Pearce, 1996). (d) Tectonic discrimination diagram for mafic rocks of Meschede (1986). WPA – within-plate alkali-basalts; WPT – within-plate tholeiites; VAB – volcanic arc basalts. (e) Chondrite-normalized REE patterns (Sun & McDonough, 1989). (f) Multi-element plot normalized to N-MORB (Sun & McDonough, 1989). Mafic units from SW Cerro Asperecito (Alasino *et al.* 2016) were added for comparison.

(ASI = 1.01–1.16) and, except for the K-feldspar-rich facies, show a decrease in TiO_2, MgO and CaO with increasing SiO_2, although the more differentiated samples show a random arrangement (Fig. 6a–c). The Na_2O does not show correlation with SiO_2 (Fig. 6d). The concentrations of some mobile trace elements are: Cs = 1.8–12 ppm; Rb = 102–319 ppm; Sr = 59–1110 ppm; and Ba = 108–1820 ppm. Rb/Ba and Rb/Sr ratios range between 0.06–2.34 and 0.09–3.27, respectively. REE concentrations normalized to chondrite (Sun & McDonough, 1989) show variable enrichment in light REEs (La_N/Yb_N = 1.4–21.1) and moderate negative Eu anomalies (Eu/Eu* = 0.35–0.81) (Fig. 6e). The multi-element plot normalized to primitive mantle (McDonough & Sun, 1995) displays negative anomalies of Nb, P, Ti and Ba, and positive anomalies of Hf, U, K and Pb (Fig. 6f).

5.b. Isotope geochemistry

5.b.1. Mafic rocks

Assuming a minimum crystallization age of 470 Ma (i.e. the peak age of the Famatinian magmatic arc, e.g. Pankhurst *et al.* 1998, 2000; Dahlquist *et al.* 2008; Ducea *et al.* 2010, 2017), the mafic rocks show a range of initial $^{87}Sr/^{86}Sr_{470}$ values of 0.70656–0.70955 and $^{143}Nd/^{144}Nd_{470}$ values of 0.511984–0.512045 (online Supplementary Table S2). The corresponding ϵNd_{470} values are between +0.24 and −0.95 (Fig. 7), and single-stage depleted mantle Nd model ages (T_{DM}) range from 1.32 to 1.74 Ga.

5.b.2. Granitoids

The granitoids (n = 8) yielded initial $^{87}Sr/^{86}Sr_{470}$ in the range 0.70562–0.71137 and $^{143}Nd/^{144}Nd_{470}$ in the range 0.511788–0.511950
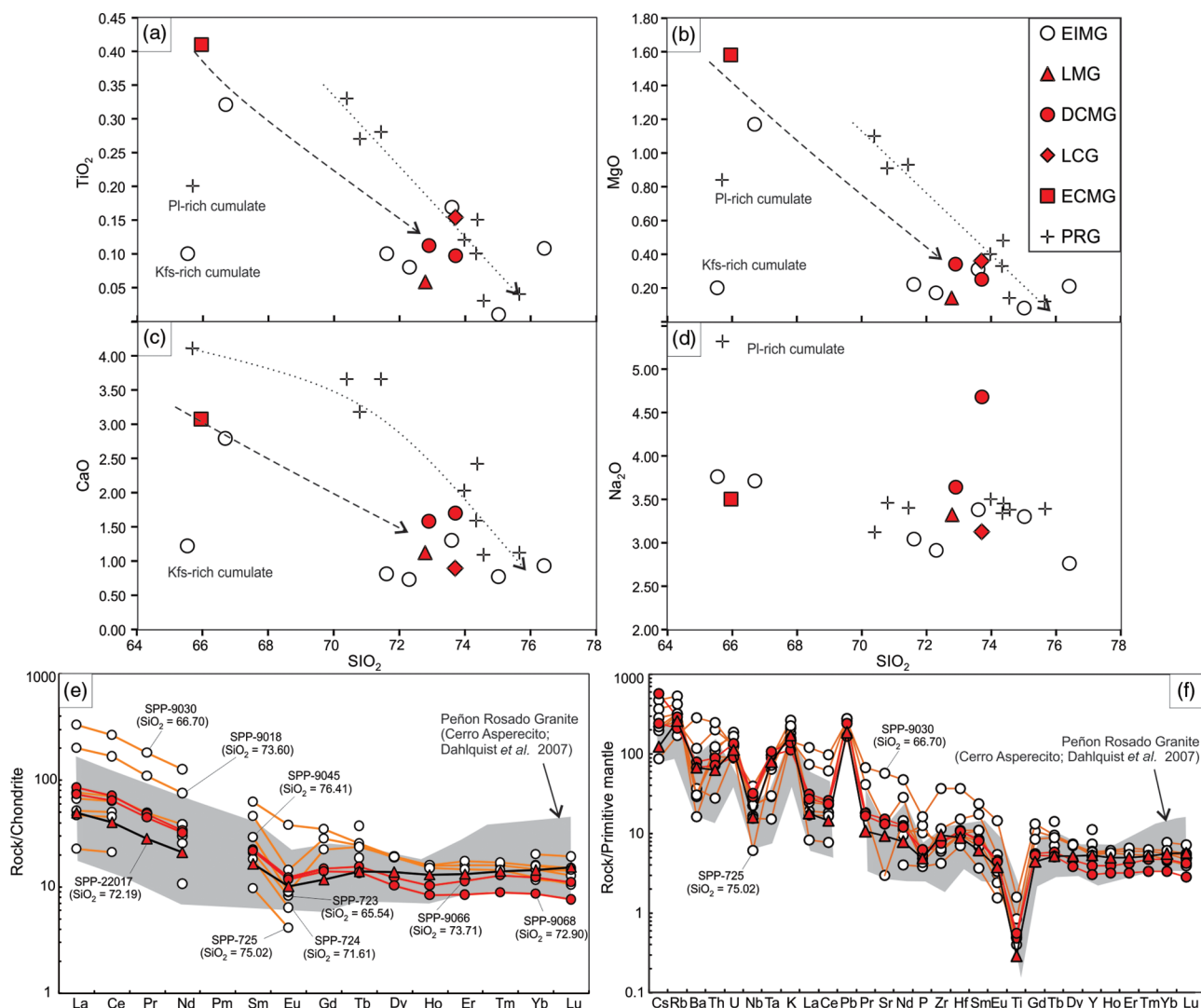
Fig. 6. (Colour online) Geochemical diagrams of granitoids from the Sierra de Pie de Palo and equivalents from elsewhere. (a–d) Harker variation diagrams showing decrease of TiO₂, MgO and CaO with increase in SiO₂, but randomly distributed in the more differentiated rocks. (e) Chondrite-normalized REE patterns (Sun & McDonough, 1989). (f) Primitive mantle normalized multi-element plot (McDonough & Sun, 1995). Peraluminous granites from the Cerro Asperecito (Peñon Rosado Granite; PRG; Dahlquist *et al.* 2007) were added for comparison. EIMG – El Indio Mylonitic Granite; LMG – Las Liebres Mylonitic Granite; DCMG – Difunta Correa Mylonitic Granite; LCG – La Chilca Granite; ECMG – El Camperito Mylonitic Granite.

(online Supplementary Table S2). The εNd₄₇₀ values vary from −1.6 to −4.78 (Fig. 7), and the Nd two-stage model ages (2*T*DM; De Paolo *et al.* 1991) are between 1.33 and 1.57 Ga.

6. U–Pb SHRIMP zircon geochronology

Only three zircon grains, 100–150 μm in length, were recovered from the low-grade metagabbrodiorite collected at Quebrada Las Flores (SPP-22004; Fig. 2). They are sub-rounded to euhedral, prismatic with bi-pyramidal terminations, and show cores and overgrowths (Fig. 8). Three spots with Th/U ratios of 0.28–0.59 yielded ages of 1812, 639 and 537 Ma (see online Supplementary Table S3). The oldest (Palaeoproterozoic) age is discordant (23%) and is from an inherited core (xenocryst). Conversely, the youngest spot corresponds to a mixed xenocryst-overgrowth age (spot 1.1; 537 ± 5 Ma; Fig. 8), and sets an upper value for the crystallization age of the metagabbrodiorite at *c*. 540 Ma.

A mylonitic granite from the Las Liebres Mylonitic Granite (SPP-22017) has zircon grains of ≤ 250 μm in length with a variety of shapes, from rounded to euhedral and prismatic with bi-pyramidal terminations (Fig. 9a). They usually show cores and large low-cathodoluminescence (low-CL) overgrowths with variable boundaries between them, from regular euhedral to irregular with resorption textures. Cores with resorbed boundaries are generally < 100 μm in length and exhibit oscillatory zoning or irregular to patchy zoning; they yielded U contents of 75–1104 ppm, and Th/U ratios of 0.06–1.45. We interpret these cores as xenocrysts partially dissolved by the magma. On the other hand, cores with euhedral boundaries are prismatic and show oscillatory zoning. They have U contents of 362–579 ppm, and Th/U ratios of 0.40–0.41 that would commonly be regarded as indicating a magmatic origin. In general, we consider Th/U ratios > 0.1 as igneous and < 0.1 as metamorphic following Rubatto (2002, 2017), although this is not always true (e.g. Pidgeon & Compston, 1992; Rubatto *et al.* 2001; Williams, 2001; Grant *et al.* 2009).
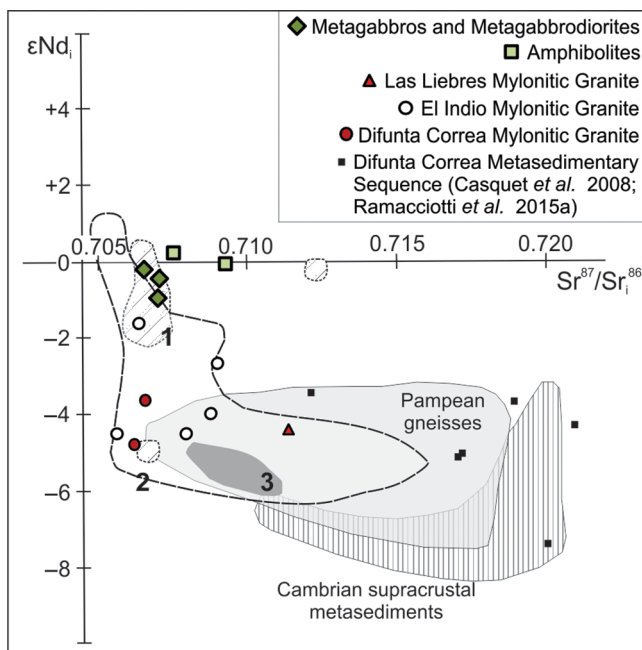
Fig. 7. (Colour online) Initial (470 Ma) isotopic composition of mafic rocks and granitoids of the Sierra de Pie de Palo and other Famatinian igneous units and metasediments of the basement of the Sierras Pampeanas. 1, SW Cerro Asperecito amphibolites (Alasino *et al.* 2016); 2, Ordovician metaluminous granitoids taken from a compilation of Alasino *et al.* (2016); 3, Cerro Asperecito peraluminous granitoids (Dahlquist *et al.* 2007). The fields of the Pampean gneisses and Cambrian supracrustal metasediments were taken from Pankhurst *et al.* (2000).

Fig. 8. (Colour online) Tera–Wasserburg diagram showing spots analysed in a few zircon grains from one metagabbrodiorite (SPP-22004) and cathodoluminiscence (CL) images. C – core; Og – overgrowth. Circles and numbers correspond to spot analysed with ages and errors at the 1σ level (see online Supplementary Table S3).

The euhedral cores are interpreted as antecrysts (see Jerram & Martin, 2008) due to the fact that their ages overlap within error with those of the overgrowths (see below). Low-CL overgrowths are euhedral prisms and internally homogeneous or with a faint oscillatory zoning; they can be large (up to 70% vol.; e.g. grain 3.1 in Fig. 9a) and yield high U contents (1329–7601 ppm) and low Th/U ratios (0.01–0.03).

Sixty spots were analysed in SPP-22017, of which 17 were discarded due to either high common Pb (> 5%), discordance (> 10%) or age error (1σ > 5%), shown as white ellipses in Figure 10a. The other ages range from 437 to 1739 Ma (online Supplementary Table S3) with a main group ($n = 9$) between 437 and 474 Ma, and a broad peak between *c*. 950 and *c*. 1300 Ma (Fig. 10b). The latter peak and the few older ages indicate inheritance (as xenocrysts) from a source, or sources, containing Mesoproterozoic and older (Palaeoproterozoic) zircons. The main group of ages (437–474 Ma) corresponds to the overgrowths and a few cores. The oldest ages within this group are from one overgrowth (spot 8.1) and from one euhedral core that we interpret as an antecryst (spot 40.1; Fig. 9a). These two spots yielded $^{206}Pb/^{238}U$ ages of 474 ± 5 Ma and 468 ± 5 Ma, respectively, which we consider close to the crystallization age of the granite (i.e. *c*. 470 Ma; similar to El Indio and Difunta Correa mylonitic granites; Baldo *et al.* 2012). With a common Pb value of 5.6%, spot 5.1 yields an age of 467 ± 5 Ma, consistent with the former two spots. The younger ages within the main group are attributed to Pb loss at ≤ 440 Ma (i.e. the youngest age found in this sample; see discussion section), which is probably related to the ductile shearing. Overgrowths are interpreted as igneous in spite of the low Th/U ratios resulting from the high U contents, which are more typical of metamorphic zircons. Similar U enrichment is reported for other weakly
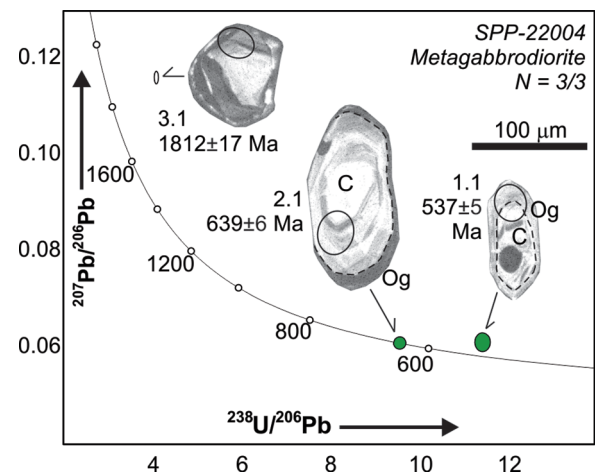
peraluminous granites (Marshall *et al.* 2011) and is related to the fractionation of Th-rich accessory minerals. The large relative volume of overgrowths along with the external idiomorphism of grains, the resorption texture of cores and the absence of evidence for metamorphic reactions involving Zr-bearing minerals in the host rock strengthen this interpretation.

A mylonitic granodiorite from the El Camperito Mylonitic Granodiorite (SPP-23023; Fig. 2) has zircon grains of ≤ 200 μm in length, with a variety of shapes from rounded to euhedral and prismatic with bi-pyramidal terminations (Fig. 9b). As in the case of SPP-22017, the zircon grains usually show cores and low-CL overgrowths, with regular euhedral to resorbed boundaries. Cores with resorbed boundaries are generally < 100 μm in length and display oscillatory or irregular and patchy zoning. The U contents are 92–1255 ppm, and the Th/U ratios range over 0.02–0.99. We interpret these cores as xenocrysts resorbed by the granodioritic magma. Cores with outer euhedral boundaries are mostly prismatic and show oscillatory zoning, with U content of 304–813 ppm and Th/U ratios of 0.54–1.4, which are commonly magmatic values. Low-CL overgrowths in this sample are volumetrically less pronounced than in SPP-22017, and yielded high U contents in the range 688–1835 ppm and Th/U ratios of 0.11–1.13.

Fifty-seven ages were obtained from SPP-23023, of which only three were discarded (white ellipses in Fig. 1c) due to high common Pb (> 5%), discordance (> 10%) or age error (1σ > 5%). The ages obtained vary over the range 432–1543 Ma (online Supplementary Table S3) with a main group ($n = 17$) of age 432–493 Ma and minor peaks at *c*. 540, 1020 and 1150 Ma (Fig. 10d). Ages of 535–561 Ma ($n = 4$) correspond to mixed core-overgrowth spots. The older cores are inherited from a Mesoproterozoic source or sources as in SPP-22017. Among the main group of ages, four grains (23.1, 11.1, 16.1 and 56.1) are for mixed core-overgrowth areas and/or plot below the Tera–Wasserburg Concordia, suggesting analytical errors. Two concordant to nearly concordant overgrowths (spots 6.1 and 10.1) yielded $^{206}Pb/^{238}U$ ages of 465 ± 5 and 472 ± 5 Ma, respectively, that we interpret as close to the crystallization age of the granodiorite (i.e. *c*. 470 Ma). The younger ages are attributed to Pb loss at ≤ 432 Ma as in sample SPP-22017. Arguments in favour of an igneous origin for the overgrowths are similar to those given for the previous sample. Remarkably,
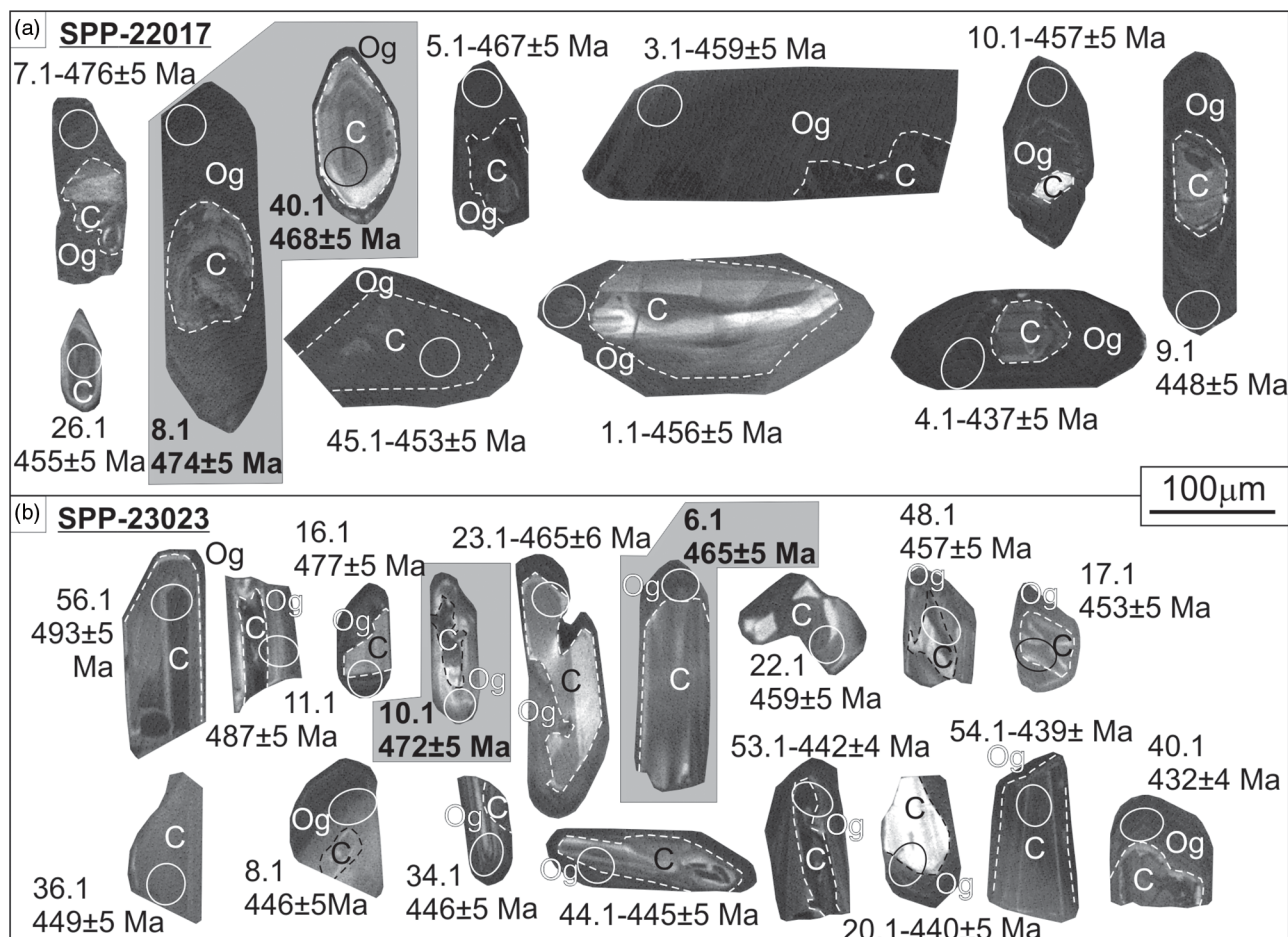
Fig. 9. Cathodoluminiscence (CL) images of the youngest zircons from the two granitoids (SPP-22017 and SPP-23023) showing cores (C) and low-CL overgrowths (Og). Zircons with shaded areas were used to infer the crystallization ages. Circles and numbers correspond to spot analyses and ages with errors at the 1σ level (see online Supplementary Table S3).

the Th/U ratios of the overgrowths in this sample are even more commonly igneous (i.e. > 0.1).

7. Discussion

7.a. Age and origin of mafic magmas

Field relationships indicate that the Sierra de Pie de Palo mafic bodies dealt with here were emplaced before regional metamorphism and earlier than the granitoids, in the form of a dyke swarm and minor stocks with gabbro to gabbrodiorite composition. These mafic magmas were emplaced mainly into the sedimentary protoliths of the Difunta Correa Metasedimentary Sequence and the Nikizanga Group, which suggests shallow intrusion. The mafic rocks further underwent low- to medium-grade metamorphism at *c.* 13 kbar, and coeval contractional deformation (F1) at 470–460 Ma (Casquet *et al.* 2001; Mulcahy *et al.* 2011; Garber *et al.* 2014). Metamorphism produced complete replacement of the primary igneous minerals, but did not significantly modify the whole-rock chemistry.

A tentative maximum crystallization age of *c.* 540 Ma was established from one mixed core-overgrowth analyses in one of the few zircons recovered from the metagabbrodiorite (SPP-22004), and is further constrained by the depositional age of the Nikizanga Group based on detrital zircon ages (490–525 Ma; Ramacciotti *et al.* 2018)

and Sr-isotope dating of the Nikizanga Group marbles (*c.* 480–510 Ma; Galindo *et al.* 2004; Ramacciotti *et al.* 2018). As regional metamorphism occurred in the Sierra de Pie de Palo at *c.* 470–460 Ma (Casquet *et al.* 2001; Mulcahy *et al.* 2011; Garber *et al.* 2014), and felsic magmatism at *c.* 470 Ma (see next section), mafic magmatism can be constrained to have occurred between *c.* 490 and 470 Ma (i.e. late Cambrian – Early Ordovician).

The geochemistry of the mafic rocks indicates that they belong to a metaluminous tholeiitic magma series. Based on the whole-rock chemical composition, two types of sources (pyroxenite and peridotite) have been proposed for the Ordovician mafic magmas in Cerro Asperecito, located north of the Sierra de Pie de Palo, and the western Famatinian Domain (Fig. 1; Alasino *et al.* 2016). The Hf/Sm and Sr/Y ratios of the analysed samples, which are useful to show whether garnet was present in the source and therefore to infer the presence of pyroxenitic sources (e.g. van Westrenen *et al.* 2001; Ducea *et al.* 2013; Lee, 2014; Liu *et al.* 2014; Murray *et al.* 2015; Alasino *et al.* 2016), exhibit values of 0.9–1.8 and 5.4–9.8, respectively. These values are closer to those of basaltic melts generated from sources dominated by olivine-orthopyroxene (Hf/Sm *c.* 0.8 and Sr/Y *c.* 4 for garnet-absent peridotite-derived melts) than those melts derived from Grt-pyroxenitic sources (Hf/Sm *c.* 0.4 and Sr/Y *c.* 15; van Westrenen *et al.* 2001; Lee *et al.* 2010; Alasino *et al.* 2016). This evidence, along with the N-MORB multi-element plot (Fig. 5f), points to a dominant
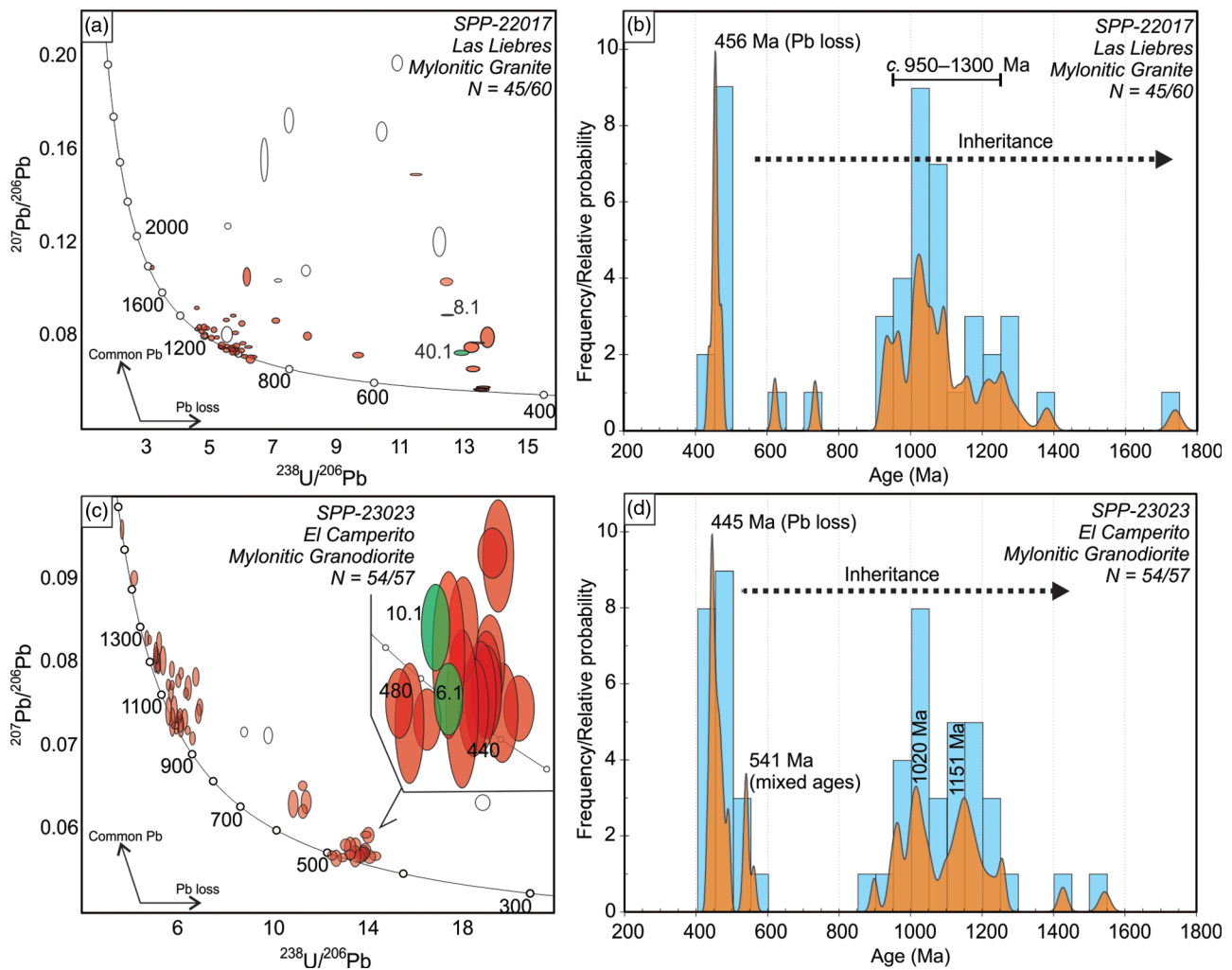
Fig. 10. (Colour online) (a, c) Tera-Wasserburg diagrams and (b, d) probability density plots of U–Pb SHRIMP zircon ages from granitoids. White ellipses in Tera-Wasserburg plots were discarded and not considered for the probability density diagrams; green ellipses correspond to the spots used to establish the crystallization age; and red ellipses to the remaining data. Error ellipses are provided at the 1σ level.

peridotite source for the primary mafic magmas of the Sierra de Pie de Palo. The same type of source was proposed for the Cerro Asperecito amphibolites (Alasino *et al.* 2016). The presence of inherited zircons in the metagabbrodiorite (SPP-22004) suggests some interaction between basaltic magma and continental crust or inheritance. However, the incorporation of earlier granitic melt fractions along the ascending pathways was not enough to significantly modify the major-element composition of the mafic magmas (i.e. less than 5% by mass; e.g. Watson, 1982; Huppert *et al.* 1985).

Because contamination with continental crust was apparently not significant, the Nd isotope composition of the mafic rocks (εNd$_{470}$ = +0.24 to −0.95) could be mainly inherited from an enriched old (Mesoproterozoic–Palaeoproterozoic) subcontinental mantle from which the continental crust was extracted. Mesoproterozoic Nd model ages similar to those found in our mafic rocks (Nd T_{DM}, 1.32–1.74 Ga) are typical of the pre-Famatinian continental crust (e.g. Casquet *et al.* 2008; Steenken *et al.* 2011; Ramacciotti *et al.* 2015*b*).

7.b. Age and origin of felsic magmas

Subsequent to the mafic plutonism, felsic magmas were emplaced. Most of these granitoid bodies were emplaced within the late-F1 El

Indio ductile thrust zone, and underwent variable contractional deformation that resulted in almost unstrained to mylonitic rocks. This magmatism occurred at *c.* 470 Ma in the Sierra de Pie de Palo (465 ± 5 to 474 ± 5 Ma), consistent with U–Pb SHRIMP ages previously reported for the El Indio Mylonitic Granite (470 ± 10 Ma) and the Difunta Correa Mylonitic Granite (474 ± 6 Ma; Baldo *et al.* 2012) and other granitic bodies within the Higueritas shear zone (470 ± 6 Ma; Mulcahy *et al.* 2011). These ages coincide, within error, with the age of regional metamorphism and thrust stacking (i.e. 470–460 Ma; Casquet *et al.* 2001; Mulcahy *et al.* 2011; Garber *et al.* 2014), suggesting, along with field evidence, syn-tectonic emplacement. The youngest ages found in overgrowths of both analysed samples (SPP-22017 and SPP-23023) probably resulted from Pb loss at *c.* 440 Ma (i.e. youngest zircons), which coincides with ^{40}Ar/^{39}Ar ages recorded by Mulcahy *et al.* (2011) from the extensional Nikizanga shear zone in the eastern side of the Sierra de Pie de Palo.

Geochemical characteristics, such as peraluminosity and negative εNd values in addition to the abundance of zircon inheritance (up to 70% of measured grains), and the presence of igneous garnet and muscovite are consistent with derivation of the felsic magmas mainly by partial melting of metasedimentary rocks (Chappell & White, 2001; online Supplmentary Tables S1 and S2).
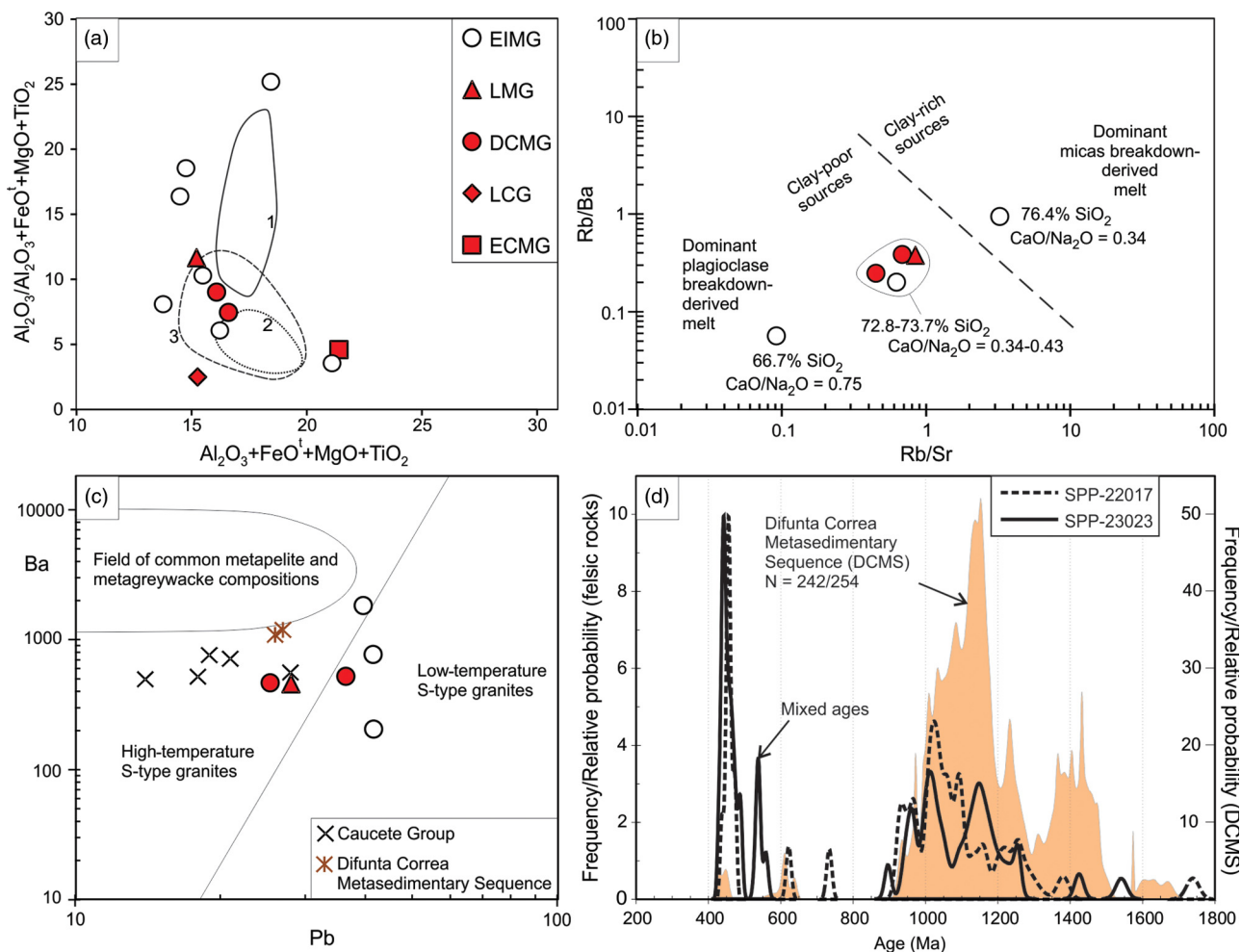
Fig. 11. (Colour online) (a) Diagram showing the relationship between alumina and mafic components (FeO^t + MgO + TiO$_2$) of the Sierra de Pie de Palo granitoids. Fields 1, 2 and 3 correspond to the composition of experimental melts derived from felsic pelites, mafic pelites and greywackes, respectively (compilation taken from Patiño Douce, 1999). (b) Rb/ Ba versus Rb/Sr diagram (after Sylvester, 1998) showing the different sources (clay-rich and clay-poor) of the Sierra de Pie de Palo granitoids. (c) Ba versus Pb diagram after Finger & Schiller (2012), suggesting that the Sierra de Pie de Palo granitoids were formed under different temperatures. Metapelites and metagreywackes compositions taken from Haak *et al.* (1984), Inger & Harris (1993), Linner (1993), Nabelek & Bartlett (1998), Solar & Brown (2001) and Rene (2006). Difunta Correa Metasedimentary Sequence data from Ramacciotti *et al.* (2015*a*) and Caucete Group from Naipauer *et al.* (2010). (d) Probability density plot of zircon ages from the two granitoids compared with a compilation of detrital zircons ages from the Difunta Correa Metasedimentary Sequence taken from Rapela *et al.* (2005) and Ramacciotti *et al.* (2015*b*).

In concordance, the Sierra de Pie de Palo granitoids show remarkably similar geochemistry to the Early–Middle Ordovician (469 ± 4 Ma) S-type granitoids (with Grt-Bt) from Cerro Asperecito in La Rioja province (Figs 6, 7; Dahlquist *et al.* 2007). The random distribution of the more differentiated samples on Harker diagrams (Fig. 6a, d) further suggest that they were not formed by fractional crystallization of a single intrusion, but multiple batches of magmas occurred. This is consistent with the high variation observed in the Sr- and Nd-isotope composition. On the other hand, the variations in alumina and mafic components (FeO^t + MgO + TiO$_2$), as well as in the Rb/Ba and Rb/Sr ratios, indicate that the source of magmas was heterogeneous (Fig. 11a, b; Sylvester, 1998; Patiño Douce, 1999). The Pb/Ba ratios – an indicator of the temperature of granitic magma formation (Finger & Schiller, 2012) – yield values corresponding to moderate (*c.* 700–780°C) to high (*c.* 800–900°C) temperature for the Sierra de Pie de Palo samples, suggesting that magmas probably derived from different crustal levels (Fig. 11c).

The Nd model ages (2T_{DM}) of the Sierra de Pie de Palo granitoids (1.33–1.57 Ga) are in the range of the T_{DM} values of the

surrounding Difunta Correa Metasedimentary Sequence (1.33–1.64 Ga; Ramacciotti *et al.* 2015*b*), representative of the pre-Famatinian continental crust. Granitic magmas could therefore have formed by partial melting of this continental crust. This is consistent with the similarities observed between the inherited zircon age patterns of the Sierra de Pie de Palo granitoids and those of the metasedimentary sequence (Fig. 11d). However, the ^{87}Sr/^{86}Sr$_i$ ratios of these granitoids (0.70561–0.71137), which are less radiogenic than the Difunta Correa Metasedimentary Sequence at 470 Ma (0.71211–0.72095; Ramacciotti *et al.* 2015*b*) and mostly similar to the mafic rocks, indicate that some degree of hybridization between crustal- and mantle- derived magmas and/or rocks probably took place at the thrust root.

7.c. Tectonic setting of magmatism

In a recent contribution Rapela *et al.* (2018) proposed that the Famatinian magmatism of the Sierras Pampeanas consists of four different domains according to their position with respect to the arc: western, central (arc), eastern and foreland domains. These

domains have distinctive geochemical and geochronological characteristics. The tectonic relationship between the central Famatinian domain and the other domains located in the east, where older igneous rocks have long been recognized (up to 490 Ma; Pankhurst *et al.* 2000), remains unknown. The western Famatinian domain includes the Sierra de Pie de Palo and SW Cerro Asperecito, among other ranges (Fig. 1a). Data presented in this work support this idea, as mafic rocks of the Sierra de Pie de Palo show geochemical and isotopic compositions similar to Ordovician deformed and metamorphosed mafic dyke swarms from SW Cerro Asperecito (Alasino *et al.* 2016), all representative of a magmatism with a tholeiitic trend (Fig. 5b, c).

The SW area of Cerro Asperecito near Villa Castelli town (see fig. 2 in Alasino *et al.* 2016) consists mainly of migmatitic gneisses and amphibolites that were originally a mafic dyke swarm (εNdt between −5 and +0.3; Nd model ages between 1.18 and 1.59 Ga; Alasino *et al.* 2016). Migmatitic gneisses contain detrital zircons of early Cambrian age (Rapela, 2000) and are probably a time-equivalent sequence to the Nikizanga Group of the Sierra de Pie de Palo.

Gabbros and diorites are also abundant in the deeper parts of the Cordilleran arc in Sierra de Valle Fértil (central Famatinian domain), and are mostly geochemically related to calc-alkaline tonalites and granodiorites that are widespread in the upper crustal levels of the arc (Pankhurst *et al.* 2000; Otamendi *et al.* 2009, 2012). Host rocks of this arc were pelitic migmatites with detrital zircon ages similiar to those of the Nikizanga Group and other post-Pampean Cambrian metasedimentary rocks further east (Ducea *et al.* 2010; Cristofolini *et al.* 2012; Rapela *et al.* 2016). Arc magmatism was largely coeval with the development of foliation, crustal thickening and high-temperature–low-pressure metamorphism resulting from advective heat at *c.* 800°C and 0.7 GPa (Dahlquist *et al.* 2005; Murra & Baldo, 2006; Gallien *et al.* 2010, 2012; Cristofolini *et al.* 2012; Tibaldi *et al.* 2013). The main phase of the arc build-up here took place over a very short time through a *c.* 4 Ma magmatic flare-up (at 472–468 Ma), as constrained by high-resolution geochronology (Ducea *et al.* 2017). An earlier tholeiitic mafic magmatic episode is however recognized in the deeper part of the arc that underwent granulite facies metamorphism with the formation of typical reaction coronas (coronitic gabbros). The pressure–temperature path was counterclockwise from *c.* 0.55 GPa and 950–1000°C to *c.* 0.7 GPa and 800°C at the pressure peak (Gallien *et al.* 2012). This earlier mafic magmatism therefore took place before both crustal thickening and main arc magmatism, and is probably correlated with the mafic rocks of the Sierra de Pie de Palo and Cerro Asperecito.

The Sierra de Pie de Palo mafic magmatism is probably equivalent to the late Cambrian – Early Ordovician allegedly extensional mafic magmatism recognized elsewhere in Sierras Pampeanas (Rossi *et al.* 1992; Mannheim & Miller, 1996; Otamendi *et al.* 2012; Dahlquist *et al.* 2013; Ducea *et al.* 2015; Alasino *et al.* 2016; Rapela *et al.* 2018).

The tectonic setting of the Sierra de Pie de Palo mafic magmatism has to be inferred from indirect evidence alone, because earlier structures were overprinted by the younger contractional phase and by the coeval moderate to high P/T metamorphism. As previously stated, mafic magmas were emplaced as shallow intrusions (a dyke swarm and small stocks) into sedimentary rocks. Moreover, mafic magmas were not differentiated by fractional crystallization or significantly contaminated by the host rocks, suggesting that the ascent to shallow levels of the crust was probably fast. Ramacciotti *et al.* (2018) proposed the existence of a

carbonate-siliciclastic platform fringing the SW Gondwana margin from Patagonia to NW Argentina during *c.* 520–490 Ma, which preceded the Famatinian subduction. In this view the continental platform collapsed when subduction started during 490–470 Ma, probably accompanied by decompression melting of the subcontinental mantle and uplift. In fact, no sedimentary rocks younger than 470 Ma are recorded in the Sierra de Pie de Palo. Because evidence of subduction-related magmatism has been recorded at *c.* 490 Ma elsewhere in the eastern Sierras Pampeanas (Rapela *et al.* 2018), we infer that the continental platform collapse started at around that age.

Sierra de Pie de Palo granitoids were emplaced at *c.* 470 Ma after the mafic magmatism during a contractional phase (F1), coeval with the Cordilleran arc magmatism (Ducea *et al.* 2017). These felsic magmas intruded into the late-F1 El Indio ductile thrust zone, the probable southern extension of the Higueritas shear zone, which was active at *c.* 470 Ma and *c.* 455 Ma (Mulcahy *et al.* 2011). The contractional phase produced crust thickening by means of folding and thrusting (Casquet *et al.* 2001, 2012). This process was accompanied by partial melting of metasedimentary rocks at the root of the El Indio ductile thrust zone. However, some hybridization with more juvenile melts and/or rocks is likely on the basis of isotope composition.

7.d. Palaeogeographic implications

Ramos *et al.* (1998) proposed merging the Pie de Palo block with the Argentine Precordillera into a larger block called Cuyania, a composite terrane immediately to the west of the Famatinian magmatic arc (i.e. west of the Bermejo fault; Fig. 1a). This block has long been considered exotic, allegedly rifted away from the Appalachian margin of Laurentia during early Cambrian time (e.g. Thomas & Astini, 1996). In this model, Cuyania was accreted to the SW Gondwana margin during Ordovician time as part of the lower plate of the Famatinian subduction (see fig. 6 in Ramos, 2004). This interpretation was challenged by several authors based on structural, geochronological and isotopic evidence (Galindo *et al.* 2004; Finney, 2007; Mulcahy *et al.* 2007, 2011; Ramacciotti *et al.* 2018). The Ordovician mafic and felsic magmatism described in this contribution can be best explained if the Sierra de Pie de Palo block was in the upper plate during the Famatinian subduction.

The Ordovician Famatinian orogen continues north in the Puna (Altiplano; Bahlburg & Hervé, 1997), northern Chile (Pankhurst *et al.* 2016), and southern and central Peru (Loewy *et al.* 2004; Chew *et al.* 2007; Casquet *et al.* 2010; Ramos, 2018). In the Puna, a forearc setting was invoked by Zimmermann *et al.* (2010) in the Cordón de Lila in Chile, outboard of the western Puna eruptive belt, long correlated with the Famatinian Cordilleran-type arc of the western Sierras Pampeanas (Bahlburg & Hervé, 1997; Pankhurst *et al.* 1998; Coira *et al.* 2009). The basin consists of a thick succession of massive basalts and a few felsic rhyolitic lavas interbedded with turbidites deposited in a marine environment. The maximun depositional age of the turbidites-based U–Pb zircon dating is 487 ± 7 Ma; rhyolitic flows yielded ages of 468 ± 6 Ma and 471 ± 6 Ma (Zimmermann *et al.* 2010). The basalts are subalkaline Fe-rich and low-K tholeiites, and rhyolites are peraluminous (Coira *et al.* 2009; Zimmermann *et al.* 2010). The maximum depositional age of the sediments, and the age of the felsic volcanic rocks are compatible with the range of ages recorded at the Sierra de Pie de Palo. We therefore speculate that sedimentary and volcanic

rocks in the Cordón de Lila, outboard of the western Puna eruptive belt, can be traced southwards, representing a shallow equivalent of the Sierra de Pie de Palo mafic and felsic magmatism.

The Famatinian orogeny has also been recognized in NE Patagonia, where plutonic rocks analogous to the Middle Ordovician granites of the Famatinian section of NW Argentina were recognized (Pankhurst *et al.* 2006, 2014). Thick metasedimentary successions were initially deposited in the Nahuel Niyeu basin during 520–510 Ma. In this case, magmatism is represented by a swarm of mafic dykes of tholeiitic chemistry that yielded a SHRIMP zircon age of 514 ± 3 Ma (Greco *et al.* 2015, 2017). This mafic magmatism in Patagonia may represent the collapse of the continental platform – and the beginning of subduction – at an earlier stage compared with the northern Pampean realm.

8. Conclusions

Mafic rocks and granitoids in the uppermost nappes of the Sierra de Pie de Palo provide information about the magmatic activity of the upper Cambrian – Lower Ordovician proto-Andean margin of Gondwana. Magmatic activity started in the Sierra de Pie de Palo as a tholeiitic mafic magmatism after deposition of the Nikizanga Group (at *c.* 490 Ma), probably related to collapse of a continental platform coeval with the beginning of subduction. Mafic magmatism preceded the regional moderate to high P/T metamorphism and the related penetrative contractional deformation. Mafic magmatism involved variable mantle sources, probably as a result of decompression melting. The older Nd-isotope model ages were probably inherited from an old Mesoproterozoic subcontinental mantle.

After tholeiitic mafic magmatism, slightly-to-moderately peraluminous granitoids were emplaced in the Sierra de Pie de Palo at *c.* 470 Ma during the contractional phase F1. This was coeval with folding, thrusting and a relatively high P/T metamorphism in the western Famatinian domain, and with development of a subduction-related Cordilleran-type magmatic arc on the east. The Sierra de Pie de Palo granitoids resulted mainly from the melting of deeply underthrusted fertile metasedimentary rocks along the El Indio ductile thrust zone, although some hybridization with more juvenile melts and/or rocks is likely on the basis of isotope composition.

The Ordovician magmatic activity shown in this paper further suggests that the Pie de Palo block was part of the upper plate during the Famatinian subduction, and not part of the exotic Precordillera terrane (lower plate).

Author ORCIDs. Carlos D. Ramacciotti, 0000-0002-0317-0019; Juan A. Dahlquist, 0000-0003-0846-7679

Supplementary material. To view supplementary material for this article, please visit https://doi.org/10.1017/S0016756819000748.

References

Aceñolaza GF and Toselli AJ (1973) Consideraciones estratigráficas y tectónicas sobre el Paleozoico Inferior del Noroeste Argentino. In *2º Congreso Latinoamericano de Geología, Caracas*, 11–16 November, pp. 755–64.

Alasino PH, Casquet C, Pankhurst RJ, Rapela CW, Dahlquist JA, Galindo C, Larrovere MA, Recio C, Paterson SR, Colombo F and Baldo EG (2016) Mafic rocks of the Ordovician Famatinian magmatic arc (NW Argentina): new insights into the mantle contribution. *Geological Society of America Bulletin* **128**, 1105–20, doi: 10.1130/B31417.1.

Astini RA, Benedetto JL and Vaccari NE (1995) The early Paleozoic evolution of the Argentine Precordillera as a Laurentian rifted, drifted and collided terrane: a geodynamic model. *Geological Society of America Bulletin* **107**, 253–73, doi: 10.1130/0016-7606(1995)107<0253:TEPEOT>2.3.CO;2.

Astini RA and Dávila FM (2004) Ordovician back arc foreland and Ocloyic thrust belt development on the western Gondwana margin as a response to Precordillera terrane accretion. *Tectonics* **23**, 1–19, doi: 10.1029/2003TC001620.

Bahlburg H and Hervé F (1997) Geodynamic evolution and tectonostratigraphic terranes of northwestern Geodynamic evolution and tectonostratigraphic terranes of northwestern Argentina and northern Chile. *Geological Society of America Bulletin* **109**, 869–84, doi: 10.1130/0016-7606(1997)109<0869.

Baldo EG, Casquet C and Galindo C (1998) Datos preliminares sobre el metamorfismo de la Sierra de Pie de Palo, *Geogaceta* **24**, 39–43.

Baldo EG, Casquet C, Pankhurst RJ, Galindo C, Rapela CW, Fanning CM, Dahlquist JA and Murra J (2006) Neoproterozoic A-type magmatism in the Western Sierras Pampeanas (Argentina): evidence for Rodinia break-up along a proto-Iapetus rift? *Terra Nova* **18**, 388–94, doi: 10.1111/j.1365-3121.2006.00703.x.

Baldo EG, Dahlquist JA, Casquet C, Rapela CW, Pankhurst RJ, Galindo C and Fanning CM (2012) Ordovician peraluminous granites in the Sierra de Pie de Palo, Western Sierras Pampeanas of Argentina: Geotectonic Implications. In *VIII Congreso Geológico de España* (eds LP Fernández, A Fernández, A Cuesta and JR Bahamonde), pp. 1907–10. Oviedo, España: CD anexo a Geo-Temas 13.

Bellahsen N, Sebrier M and Siame L (2016) Crustal shortening at the Sierra Pie de Palo (Sierras Pampeanas, Argentina): near-surface basement folding and thrusting. *Geological Magazine* **153**, 992–12, doi: 10.1017/S0016756816000467.

Borello AV (1969) Los geosinclinales de la Argentina: Buenos Aires, Dirección Nacional de Geología y Minería. *Anales* **14**, 1–36.

Büttner SH, Glodny J, Lucassen F, Wemmer K, Erdmann S, Handler R and Franz G (2005) Ordovician metamorphism and plutonism in the Sierra de Quilmes metamorphic complex: Implications for the tectonic setting of the northern Sierras Pampeanas (NW Argentina). *Lithos* **83**, 143–81, doi: 10.1016/j.lithos.2005.01.006.

Casquet C, Baldo EG, Pankhurst RJ, Rapela CW, Galindo C, Fanning CM and Saavedra J (2001) Involvement of the Argentine Precordillera terrane in the Famatinian mobile belt: U-Pb SHRIMP and metamorphic evidence from the Sierra de Pie de Palo. *Geology* **29**, 703–06, doi: 10.1130/0091-7613(2001)029<0703:IOTAPT>2.0.CO;2.

Casquet C, Pankhurst RJ, Rapela CW, Galindo C, Fanning CM, Chiaradia M, Baldo EG, González-Casado JM and Dahlquist JA (2008) The Mesoproterozoic Maz terrane in the Western Sierras Pampeanas, Argentina, equivalent to the Arequipa-Antofalla block of southern Peru? Implications for West Gondwana margin evolution. *Gondwana Research* **13**, 163–75, doi: 10.1016/j.gr.2007.04.005.

Casquet C, Fanning CM, Galindo C, Pankhurst RJ, Rapela CW and Torres P (2010) The Arequipa Massif of Peru: New SHRIMP and isotope constraints on a Paleoproterozoic inlier in the Grenvillian orogen. *Journal of South American Earth Sciences* **29**, 128–42, doi: 10.1016/j.jsames.2009.08.009.

Casquet C, Rapela CW, Pankhurst RJ, Baldo EG, Galindo C, Fanning CM and Dahlquist JA (2012) Fast sediment underplating and essentially coeval juvenile magmatism in the Ordovician margin of Gondwana, Western Sierras Pampeanas, Argentina. *Gondwana Research* **22**, 664–73, doi: 10.1016/j.gr.2012.05.001.

Cawood PA (2005) Terra Australis Orogen: Rodinia breakup and development of the Pacific and Iapetus margins of Gondwana during the Neoproterozoic and Paleozoic. *Earth-Science Reviews* **69**, 249–79, doi: 10.1016/j.earscirev.2004.09.001.

Cawood PA, Kroner A, Collins WJ, Kusky TM, Mooney WD and Windley BF (2009) Accretionary orogens through Earth history. In *Earth Accretionary Systems in Space and Time* (eds PA Cawood and A Kröner), pp. 1–36. Geological Society, London, Special Publications no. 318, doi: 10.1144/SP318.1.

Chappell BW and White JR (2001) Two contrasting granite types: 25 years later. *Australian Journal of Earth Sciences* **48**, 489–99, doi: 10.1046/j.1440-0952.2001.00882.x.

Chew DM, Schaltegger, U, Košler, J, Whitehouse MJ, Gutjahr, M, Spikings RA and Miškovic, A (2007) U-Pb geochronologic evidence for the evolution of the Gondwanan margin of the north-central Andes. *Journal of the Geological Society, London* **119**, 697–11, doi: 10.1130/B26080.1.

Coira B, Koukharsky, M, Guevara SR and Cisterna CE (2009) Puna (Argentina) and northern Chile Ordovician basic magmatism: a contribution to the tectonic setting. *Journal of South American Earth Sciences* **27**, 24–35, doi: 10.1016/j.jsames.2008.10.002.

Cristofolini EA, Otamendi JE, Ducea MN, Pearson DM, Tibaldi AM and Baliani I (2012) Detrital zircon U-Pb ages of metasedimentary rocks from Sierra de Valle Fértil: Entrapment of Middle and Late Cambrian marine successions in the deep roots of the Early Ordovician Famatinian arc. *Journal of South American Earth Sciences* **37**, 77–94, doi: 10.1016/j.jsames.2012.02.001.

Dahlquist JA, Galindo C, Pankhurst RJ, Rapela CW, Alasino PH, Saavedra J and Fanning CM (2007) Magmatic evolution of the Peñón Rosado granite: Petrogenesis of garnet-bearing granitoids, *Lithos* **95**, 177–07, doi: 10.1016/j.lithos.2006.07.010.

Dahlquist JA, Pankhurst RJ, Gaschnig RM, Rapela CW, Casquet C, Alasino PH, Galindo C and Baldo EG (2013) Hf and Nd isotopes in Early Ordovician to Early Carboniferous granites as monitors of crustal growth in the Proto-Andean margin of Gondwana. *Gondwana Research* **23**, 1617–30, doi: 10.1016/j.gr.2012.08.013.

Dahlquist JA, Pankhurst RJ, Rapela CW, Galindo C, Alasino PH, Fanning CM, Saavedra J and Baldo EG (2008) New SHRIMP U-Pb data from the Famatina Complex: Constraining Early-Mid Ordovician Famatinian magmatism in the Sierras Pampeanas, Argentina. *Geologica Acta* **6**, 319–33, doi: 10.1344/105.000000260.

Dahlquist JA, Rapela CW and Baldo EG (2005) Petrogenesis of cordierite-bearing S-type granitoids in Sierra de Chepes, Famatinian orogen, Argentina. *Journal of South American Earth Sciences* **20**, 231–51, doi: 10.1016/j.jsames.2005.05.014.

De Paolo DJ, Linn AM and Schubert G (1991) The continental crustal age distribution: Methods of determining mantle separation ages from Sm-Nd isotopic data and application to the southwestern United States. *Journal of Geophysical Research* **96**, 2071–88, doi: 10.1029/90JB02219.

Drobe M, López de Luchi M Steenken A, Wemmer K, Naumann R, Frei R and Siegesmund S (2011) Geodynamic evolution of the Eastern Sierras Pampeanas (Central Argentina) based on geochemical, Sm-Nd, Pb-Pb and SHRIMP data. *International Journal of Earth Sciences* **100**, 631–57, doi: 10.1007/s00531-010-0593-3.

Ducea MN, Bergantz GW, Crowley JL and Otamendi JE (2017) Ultrafast magmatic buildup and diversification to produce continental crust during subduction. *Geology* **45**, 235–238, doi: 10.1130/G38726.1.

Ducea MN, Otamendi JE, Bergantz GW, Jianu D and Petrescu L (2015) The origin and petrologic evolution of the Ordovician Famatinian-Puna arc. In *Geodynamics of a Cordilleran Orogenic System: The Central Andes of Argentina and Northern Chile* (eds PG DeCelles, MN Ducea, B Carrapa and PA Kapp), pp. 125–38. Geological Society of America, Boulder, Memoir no. 212, doi:10.1130/2015.1212(07).

Ducea MN, Otamendi JE, Bergantz GW, Stair KM, Valencia VA and Gehrels GE (2010) Timing constraints on building an intermediate plutonic arc crustal section: U-Pb zircon geochronology of the Sierra Valle Fértil-La Huerta, Famatinian arc, Argentina. *Tectonics* **29**, TC4002, doi: 10.1029/2009TC002615.

Ducea MN, Seclaman AC, Murray KE, Jianu D and Schoenbohm LM (2013) Mantle-drip magmatism beneath the Altiplano-Puna Plateau, Central Andes. *Geology* **41**, 915–18, doi: 10.1130/G34509.1.

Faure G (2001) *Origin of Igneous Rocks: The Isotopic Evidence.* Heidelberg: Springer-Verlag, 496 p. doi: 10.1007/978-3-662-04474-2.

Finger F and Schiller D (2012) Lead contents of S-type granites and their petrogenetic significance. *Contribution to Mineralogy Petrology* **164**, 747–55, doi: 10.1007/s00410-012-0771-3.

Finney SC (2007) The parautochthonous Gondwanan origin of the Cuyania (greater Precordillera) terrane of Argentina: a re-evaluation of evidence used to support an allochthonous Laurentian origin. *Geologica Acta* **5**, 127–58.

Galindo C, Casquet C, Rapela CW, Pankhurst RJ, Baldo EG and Saavedra J (2004) Sr, C and O isotope geochemistry and stratigraphy of Precambrian and lower Paleozoic carbonate sequences from the Western Sierras Pampeanas of Argentina: Tectonic implications. *Precambrian Research* **131**, 55–71, doi: 10.1016/j.precamres.2003.12.007.

Gallien F, Mogessie A, Bjerg E, Delpino S, Castro de Machuca B, Thöni M and Klötzli U (2010) Timing and rate of granulite facies metamorphism and cooling from multi-mineral chronology on migmatitic gneisses, Sierras de La Huerta and Valle Fértil NW Argentina. *Lithos* **114**, 229–52, doi: 10.1016/j.lithos.2009.08.011.

Gallien F, Mogessie A, Hauzenberger CA, Bjerg E, Delpino S and Castro de Machuca B (2012) On the origin of multi-layer coronas between olivine and plagioclase at the gabbro-granulite transition, Valle Fértil-La Huerta Ranges, San Juan Province, Argentina. *Journal of Metamorphic Geology* **30**, 281–02, doi: 10.1111/j.1525-1314.2011.00967.x.

Garber JM, Roeske SM, Warren J, Mulcahy SR, McClelland WC, Austin LJ, Renne PR and Vujovich GI (2014) Crustal shortening, exhumation, and strain localization in a collisional orogen: The Bajo Pequeño Shear Zone, Sierra de Pie de Palo, Argentina. *Tectonics* **33**, 1277–03, doi: 10.1002/2013TC003477.

Goldstein SL, O'Nions RK and Hamilton PJ (1984) A Sm-Nd study of atmospheric dust and particles from major river systems. *Earth and Planetary Science Letters* **70**, 221–36.

Grant ML, Wilde SA, Wu F and Yang J (2009) The application of zircon cathodoluminescence imaging, Th–U–Pb chemistry and U–Pb ages in interpreting discrete magmatic and high-grade metamorphic events in the North China Craton at the Archean/Proterozoic boundary. *Chemical Geology* **261**, 155–71, doi: 10.1016/j.chemgeo.2008.11.002.

Greco GA, González PD, González SN, Sato AM, Basei MAS, Tassinari CCG, Sato K, Varela R and Llambías EJ (2015) Geology, structure and age of the Nahuel Niyeu Formation in the Aguada Cecilio area, North Patagonian Massif, Argentina. *Journal of South American Earth Sciences* **62**, 12–32, doi: 10.1016/j.jsames.2015.04.005.

Greco GA, González SN, Sato AM, González PD, Basei MAS, Llambías EJ and Varela R (2017) The Nahuel Niyeu basin: A Cambrian forearc basin in the eastern North Patagonian Massif. *Journal of South American Earth Sciences* **79**, 111–36, doi: 10.1016/j.jsames.2017.07.009.

Grosse P, Bellos LI, de los Hoyos CR, Larrovere MA, Rossi JN and Toselli AJ (2011) Across-arc variation of the Famatinian magmatic arc (NW Argentina) exemplified by I-, S- and transitional I/S-type Early Ordovician granitoids of the Sierra de Velasco. *Journal of South American Earth Sciences* **32**, 110–26, doi: 10.1016/j.jsames.2011.03.014.

Haak U, Heinrichs H, Boneß M and Schneider A (1984) Loss of metals from pelites during regional metamorphism. *Contribution to Mineralogy and Petrology* **85**, 116–32.

Huppert HE, Stephen R and Sparks J (1985) Cooling and contamination of mafic and ultramafic magmas during ascent through continental crust. *Earth and Planetary Science Letters* **74**, 371–86, doi: 10.1016/S0012-821X(85)80009-1.

Inger S and Harris N (1993) Leucogranite magmatism in the Langtang Valley. *Journal of Petrology* **34**, 345–68.

Jacobsen SB and Wasserburg GJ (1980) Sm-Nd isotopic evolution of chondrites, *Earth and Planetary Science Letters* **50**, 139–55.

Jerram DA and Martin VM (2008) Understanding crystal populations and their significance through the magma plumbing system. In *Dynamics of Crustal Magma Transfer, Storage and Differentiation* (eds C Annen and GF Zellmer), pp. 133–48. Geological Society of London, Special Publications no. 304, doi: 10.1144/SP304.7.

Jordan TE and Allmendinger RW (1986) The Sierras Pampeanas of Argentina: a modern analogue of Rocky Mountain foreland deformation. *American Journal of Science* **286**, 737–64, doi: 10.2475/ajs.286.10.737.

Kopp H (2013) Invited review paper: The control of subduction zone structural complexity and geometry on margin segmentation and seismicity. *Tectonophysics* **589**, 1–16, doi: 10.1016/j.tecto.2012.12.037.

Lee C-TA (2014) Physics and chemistry of deep continental crust recycling. In *Treatise on Geochemistry* (2nd ed.), Volume **4** (eds H Holland and K Turekian), pp. 423–56. Elsevier. doi: 10.1016/B978-0-08-095975-7.00314-4.

Lee C-TA, Luffi P, Le Roux V, Dasgupta R, Albaréde F and Leeman WP (2010) The redox state of arc mantle using Zn/Fe systematics. *Nature* **468**, 681–85, doi: 10.1038/nature09617.

Linner M (1993) Zur Geochemie der Paragneise in der Monotonen Serie. *Mitteilungen der Österreichischen Mineralogischen Gesellschaft* **138**, 223–25.

Liu C-Z, Wu F-Y, Chung S-L, Sun W-D and Ji WQ (2014) A 'hidden' ^{18}O-enriched reservoir in the sub-arc mantle. *Scientific Reports* **4**, 4232, doi: 10.1038/srep04232.

Loewy SL, Connelly JN and Dalziel IWD (2004) An orphaned basement block: The Arequipa-Antofalla Basement of the central Andean margin of South America. *Geological Society of America Bulletin* **116**, 171–87, doi: 10.1130/B25226.1.

Ludwig KR (2003) *Isoplot/Ex version 3.0: A Geochronological Toolkit for Microsoft Excel*. Berkeley, California: Berkeley Geochronology Center, Special Publication No. 4

Lugmair GW and Carlson RW (1978) The Sm-Nd history of KREEP. In *Proceedings of 9th Lunar and Planetary Science Conference*, Houston, 13–17 March, 689–04.

Lugmair GW and Marti K (1978) Lunar initial 143Nd/144 Nd: differential evolution of the lunar crust and mantle. *Earth and Planetary Science Letters* **39**, 349–57.

Malavieille J and Trullenque G (2009) Consequences of continental subduction on forearc basin and accretionary wedge deformation in SE Taiwan: Insights from analogue modeling. *Tectonophysics* **466**, 377–94, doi: 10.1016/j.tecto.2007.11.016.

Mannheim R and Miller H (1996) Las rocas volcánicas y subvolcánicas eopaleozoicas del Sistema de Famatina. *Münchner Geologische Hefte* **19A**, 159–86.

Marshall V, Knesel K and Bryan SE (2011) Zircon chronochemistry of high heat-producing granites in Queensland and Europe. In *Australian Geothermal Energy Conference* (ed. A Budd), Sydney, Australia, 16–18 November, pp. 157–64.

McDonough WF and Sun S (1995) The composition of the Earth. *Chemical Geology* **120**, 223–53.

Meschede M (1986) A method of discriminating between different types of mid-ocean ridge basalts and continental tholeiites with the Nb-Zr-Y diagram. *Chemical Geology* **56**, 207–18, doi: 10.1016/0009-2541(86)90004-5.

Michard A, Gurriet P, Soudant M and Abarede F (1985) Nd isotopes in French Phanerozoic shales: external vs internal aspect of crust evolution. *Geochimica and Cosmochimica Acta* **49**, 601–10.

Miyashiro A (1974) Volcanic rock series in island arcs and active continental margins. *American Journal of Science* **274**, 321–55.

Morata D, Castro de Machuca B, Arancibia G, Pontoriero S and Fanning CM (2010) Peraluminous Grenvillian TTG in the Sierra de Pie de Palo, Western Sierras Pampeanas, Argentina: Petrology, geochronology, geochemistry and petrogenetic implications. *Precambrian Research* **177**, 308–22, doi: 10.1016/j.precamres.2010.01.001.

Mulcahy SR, Roeske SM, McClelland WC, Ellis JR, Jourdan F, Renne PR, Vervoort JD and Vujovich GI (2014) Multiple migmatite events and cooling from granulite facies metamorphism within the Famatina arc margin of northwest Argentina. *Tectonics* **33**, 1–25, doi: 10.1002/2013TC003398.

Mulcahy SR, Roeske SM, McClelland WC, Jourdan F, Iriondo A, Renne PR, Vervoort JD and Vujovich GI (2011) Structural evolution of a composite middle to lower crustal section: The Sierra de Pie de Palo, northwest Argentina. *Tectonics* **30**, doi: 10.1029/2009TC002656.

Mulcahy SR, Roeske SM, McClelland WC, Nomade S and Renne PR (2007) Cambrian initiation of the Las Pirquitas thrust of the western Sierras Pampeans, Argentina: Implications for the tectonic evolution of the proto-Andean margin of South America. *Geology* **35**, 443–46, doi: 10.1130/G23436A.1.

Murra JA and Baldo EG (2006) Evolución tectonotermal ordovícica del borde occidental del arco magmático Famatiniano: metamorfismo de las rocas máficas y ultramáficas de la Sierra de la Huerta-de Las Imanas (Sierras Pampeanas, Argentina). *Revista geológica de Chile* **33**, 277–98, doi: 10.4067/S0716-02082006000200004.

Murray KE, Ducea MN and Schoenbohm L (2015) Foundering-driven lithospheric melting: The source of central Andean mafic lavas on the Puna Plateau (22°S–27°S). In *Geodynamics of a Cordilleran Orogenic System: The Central Andes of Argentina and Northern Chile* (eds PG DeCelles, MN Ducea, B Carrapa and Kapp PA), pp. 139–66. Geological Society of America, Boulder, Memoir no. 212.

Nabelek PI and Bartlett CD (1998) Petrologic and geochemical links between the post-collisional Proterozoic Harney Peak leucogranite, South Dakota USA, and its source rocks. *Lithos* **45**, 71–85.

Naipauer M, Cingolani CA, Vujovich GI and Chemale F (2010) Geochemistry of Neoproterozoic-Cambrian metasedimentary rocks of the Caucete Group, Sierra de Pie de Palo, Argentina: Implications for their provenance. *Journal of South American Earth Sciences* **30**, 84–96, doi: 10.1016/j.jsames.2010.03.002.

Otamendi JE, Ducea MN and Bergantz GW (2012) Geological, petrological and geochemical evidence for progressive construction of an arc crustal section, Sierra de Valle Fértil, Famatinian Arc, Argentina. *Journal of Petrology* **53**, 761–00, doi: 10.1093/petrology/egr079.

Otamendi JE, Ducea MN, Tibaldi AM, Bergantz GW, de la Rosa JD and Vujovich GI (2009) Generation of tonalitic and dioritic magmas by coupled partial melting of gabbroic and metasedimentary rocks within the deep crust of the Famatinian magmatic arc, Argentina. *Journal of Petrology* **50**, 841–73, doi: 10.1093/petrology/egp022.

Pankhurst RJ and O'Nions RK (1973) Determination of Rb/Sr and 87Sr/86Sr ratios of some standard rocks and evaluation of X-ray fluorescence spectrometry in Rb-Sr geochemistry. *Chemical Geology* **12**, 127–36, doi: 10.1016/0009-2541(73)90110-1.

Pankhurst RJ and Rapela CW (1998) The proto-Andean margin of Gondwana: an introduction. In *The Proto-Andean Margin of Gondwana* (eds RJ Pankhurst and WC Rapela), pp. 1–9. Geological Society of London, Special Publication no. 142.

Pankhurst RJ, Hervé F, Fanning CM, Calderón M, Niemeyer H, Griem-Klee S and Soto F (2016) The pre-Mesozoic rocks of northern Chile: U-Pb ages, and Hf and O isotopes. *Earth-Science Reviews* **152**, 88–05, doi: 10.1016/j.earscirev.2015.11.009.

Pankhurst RJ, Rapela CW and Fanning CM (2000) Age and origin of coeval TTG, I- and S-type granites in the Famatinian belt of NW Argentina. *Transactions of the Royal Society of Edinburgh: Earth Sciences* **91**, 151–68, doi: 10.1017/S0263593300007343.

Pankhurst RJ, Rapela CW, Fanning CM and Márquez M (2006) Gondwanide continental collision and the origin of Patagonia. *Earth-Science Reviews* **76**, 235–57, doi: 10.1016/j.earscirev.2006.02.001.

Pankhurst RJ, Rapela CW, Lopez De Luchi MG, Rapalini AE, Fanning CM and Galindo C (2014) The Gondwana connections of northern Patagonia. *Journal of the Geological Society of London* **171**, 313–28, doi: 10.1144/jgs2013-081.

Pankhurst RJ, Rapela CW, Saavedra J, Baldo EG, Dahlquist JA, Pascua I and Fanning CM (1998) The Famatinian magmatic arc in the central Sierras Pampeanas: an Early-to-Middle Ordovician continental arc on the Gondwana margin. In *The Proto-Andean Margin of Gondwana* (eds RJ Pankhurst and CW Rapela), pp. 343–67. Geological Society of London, Special Publication no. 142.

Patiño Douce AE (1999) What do experiments tell us about the relative contributions of crust and mantle to the origin of granitic magmas? In *Understanding Granites: Integrating New and Classical Techniques* (eds A Castro, C Fernández and JL Vigneresse), pp. 55–75. Geological Society of London, Special Publication no. 168.

Pearce JA (1996) A user's guide to basalt discrimination diagrams. In *Trace Element Geochemistry of Volcanic Rocks: Applications for Massive Sulphide Exploration* (ed DA Wyman), pp. 79–13, St Johns: Geological Association of Canada, Short Course Notes, Vol. 12.

Pidgeon RT and Compston W (1992) A SHRIMP ion microprobe study of inherited and magmatic zircons from four Scottish Caledonian granites.

Transactions of the Royal Society of Edinburgh: Earth Sciences **83**, 473–83, doi: 10.1017/S0263593300008142.

Ramacciotti CD, Baldo EG and Casquet C (2015a) U-Pb SHRIMP detrital zircon ages from the Neoproterozoic Difunta Correa Metasedimentary Sequence (Western Sierras Pampeanas, Argentina): Provenance and paleogeographic implications. *Precambrian Research* **270**, 39–49, doi: 10.1016/j.precamres.2015.09.008.

Ramacciotti CD, Casquet C, Baldo EG and Galindo C (2015b) The Difunta Correa metasedimentary sequence (NW Argentina): relict of a Neoproterozoic platform? Elemental and Sr-Nd isotope evidence. *Revista Mexicana de Ciencias Geologicas* **32**, 395–14.

Ramacciotti CD, Casquet C, Baldo EG, Galindo C, Pankhurst RJ, Verdecchia SO, Rapela CW and Fanning MC (2018) A Cambrian mixed carbonate-siliciclastic platform in SW Gondwana: evidence from the Western Sierras Pampeanas (Argentina) and implications for the early Paleozoic paleogeography of the proto-Andean margin. *International Journal of Earth Sciences* **107**, 2605–25, doi: 10.1007/s00531-018-1617-7.

Ramos VA (1988) Late Proterozoic-Early Paleozoic of South America – a collisional history. *Episodes* **11**, 168–74.

Ramos VA (2004) Cuyania, an exotic block to Gondwana: Review of a historical success and the present problems. *Gondwana Research* **7**, 1009–26, doi: 10.1016/S1342-937X(05)71081-9.

Ramos VA (2018) The Famatinian orogen along the protomargin of Western Gondwana: Evidence for a nearly continuous Ordovician magmatic arc between Venezuela and Argentina. In *The Evolution of the Chilean-Argentinean Andes* (eds A Folguera, E Contreras Reyes, N Heredia, A Encinas, BS Iannelli, V Oliveros, FM Dávila, G Collo, L Giambiagi, A Maksymowicz, MP Iglesia Llanos, M Turienzo, M Naipauer, D Orts, VD Litvak, O Alvarez and C Arriagada), pp. 133–61. Switzerland: Springer.

Ramos VA, Dallmeyer RD and Vujovich GI (1998) Time constraints on the Early Paleozoic docking of the Precordillera, central Argentina. In *The Proto-Andean Margin of Gondwana* (eds RJ Pankhurst and CW Rapela), pp. 143–58. London: Geological Society of London, Special Publication no. 142.

Ramos VA and Vujovich GI (2000) *Hoja Geológica 3169-VI. San Juan*, **243**. Boletín, Buenos Aires: Servicio Geológico Minero Argentino, 82 pp.

Rapela CW (2000) El ambiente geotectónico del Ordovícico de la región del Famatina. *Revista de la Asociacion Geologica Argentina* **55**, 134–36.

Rapela CW, Pankhurst RJ, Casquet C, Baldo EG, Galindo C, Fanning CM and Dahlquist JA (2010) The Western Sierras Pampeanas: Protracted Grenville-age history (1330-1030 Ma) of intra-oceanic arcs, subduction-accretion at continental-edge and AMCG intraplate magmatism. *Journal of South American Earth Sciences* **29**, 105–27, doi: 10.1016/j.jsames.2009.08.004.

Rapela CW, Pankhurst RJ, Casquet C, Baldo EG, Saavedra J and Galindo C (1998) Early evoution of the Proto- Andean margin of South America. *Geology* **26**, 707–10, doi: 10.1130/0091-7613(1998)026<0707:EEOTPA>2.3.CO.

Rapela CW, Pankhurst RJ, Casquet C, Dahlquist JA, Fanning CM, Baldo EG, Galindo C, Alasino PH, Ramacciotti CD, Verdecchia SO, Murra JA and Basei MAS (2018) A review of the Famatinian Ordovician magmatism in southern South America: evidence of lithosphere reworking and continental subduction in the early proto-Andean margin of Gondwana. *Earth-Science Reviews* **187**, 259–85.

Rapela CW, Pankhurst RJ, Casquet C, Fanning CM, Baldo EG, González-Casado JM, Galindo C and Dahlquist JA (2007) The Río de la Plata craton and the assembly of SW Gondwana. *Earth-Science Reviews* **83**, 49–82, doi: 10.1016/j.earscirev.2007.03.004.

Rapela CW, Pankhurst RJ, Casquet C, Fanning CM, Galindo C and Baldo EG (2005) Datación U-Pb SHRIMP de circones detríticos en paranfibolitas neoproterozoicas de la secuencia Difunta Correa (Sierras Pampeanas Occidentales, Argentina). *Geogaceta* **38**, 227–30.

Rapela CW, Verdecchia SO, Casquet C, Pankhurst RJ, Baldo EG, Galindo C, Murra JA, Dahlquist JA and Fanning CM (2016) Identifying Laurentian and SW Gondwana sources in the Neoproterozoic to Early Paleozoic metasedimentary rocks of the Sierras Pampeanas: Paleogeographic and tectonic implications. *Gondwana Research* **32**, 193–12, doi: 10.1016/j.gr.2015.02.010.

Rene M (2006) Provenance studies of Moldanubian paragneisses based on geochemical data (Bohemian Massif, Czech Republic). *Neues Jahrbuch für Geologie Abhandlungen* **242**, 83–01.

Rossi JN, Toselli AJ and Durand FR (1992) Metamorfismo de baja presión, su relación con el desarrollo de la cuenca Puncoviscana, plutonismo y régimen tectónico. *Estudios Geológicos* **48**, 279–87.

Rubatto D (2002) Zircon trace element geochemistry: distribution coefficients and the link between U-Pb ages and metamorphism. *Chemical Geology* **184**, 123–38.

Rubatto D (2017) Zircon: The metamorphic mineral. In *Petrochronology: Methods and Applications* (eds MJ Kohn, M Engi and P Lanari), pp. 261–95. *Reviews in Mineralogy & Geochemistry* **83**.

Rubatto D, Williams IS and Buick IS (2001) Zircon and monazite response to prograde metamorphism in the Reynolds Range, central Australia. *Contributions to Mineralogy and Petrology* **140**, 458–68, doi: 10.1007/PL00007673.

Sims JP, Ireland TR, Camacho A, Lyons P, Pieters PE, Skirrow RG, Stuart-Smith PG and Mrió R (1998) U-Pb, Th-Pb and Ar-Ar geochronology from the southern Sierras Pampeanas, Argentina: implications for the Paleozoic tectonic evolution of the western Gondwana margin. In *The Proto-Andean margin of Gondwana* (eds RJ Pankhurst and CW Rapela), pp. 259–82. Geological Society of London, Special Publication no. 142.

Solar GS and Brown M (2001) Petrogenesis of migmatites in Maine USA: possible source of peraluminous leucogranite in plutons? *Journal of Petrology* **42**, 789–23.

Steenken A, López de Luchi MG, Dopico CM, Drobe M, Wemmer K and Siegesmund S (2011) The Neoproterozoic-early Paleozoic metamorphic and magmatic evolution of the Eastern Sierras Pampeanas: an overview. *International Journal of Earth Sciences* **100**, 465–88, doi: 10.1007/s00531-010-0624-0.

Steenken A, Siegesmund S, López de Luchi MG, Frei R and Wemmer K (2006) Neoproterozoic to Early Palaeozoic events in the Sierra de San Luis: implications for the Famatinian geodynamics in the Eastern Sierras Pampeanas (Argentina). *Journal of the Geological Society of London* **163**, 965–82.

Sun S and McDonough WF (1989) Chemical and isotopic systematics of oceanic basalts: implication for mantle composition and processes. In *Magmatism in the Ocean Basins* (eds AD Saunders and MJ Norry), pp. 313–45. Geological Society of London, Special Publication no. 42.

Sylvester PJ (1998) Post-collisional strongly peraluminous granites. *Lithos* **45**, 29–44.

Thomas WA and Astini RA (1996) The Argentine Precordillera: A traveler from the Ouachita Embayment of North American Laurentia. *Science* **273**, 752–57.

Tibaldi AM, Otamendi JE, Cristofolini EA, Baliani I, Walker BA and Berganz GW (2013) Reconstruction of the Early Ordovician Famatinian arc through thermobarometry in lower and middle crustal exposures, Sierra de Valle Fértil, Argentina. *Tectonophysics* **589**, 151–66, doi: 10.1016/j.tecto.2012.12.032.

van Staal CR, Vujovich GI, Currie KL and Naipauer M (2011) An Alpine-style Ordovician collision complex in the Sierra de Pie de Palo, Argentina: Record of subduction of Cuyania beneath the Famatina arc. *Journal of Structural Geology* **33**, 343–61, doi: 10.1016/j.jsg.2010.10.011.

van Westrenen W, Blundy JD and Wood BJ (2001) High field strength element/rare earth element fractionation during partial melting in the presence of garnet: Implications for identification of mantle heterogeneities. *Geochemistry, Geophysics, Geosystems* **2**, doi: 10.1029/2000GC000133.

Vujovich GI and Kay SM (1998) A Laurentian? Grenville-age oceanic arc/back-arc terrane in the Sierra de Pie de Palo, Western Sierras Pampeanas, Argentina. In *The Proto-Andean Margin of Gondwana* (eds RJ Pankhurst and CW Rapela), pp. 159–79. Geological Society of London, Special Publication no. 142, doi: 10.1144/GSL.SP.1998.142.01.09.

Vujovich GI, van Staal CR and Davis W (2004) Age constraints on the tectonic evolution and provenance of the Pie de Palo Complex, Cuyania composite terrane, and the Famatinian Orogeny in the Sierra de Pie de Palo, San Juan, Argentina. *Gondwana Research* **7**, 1041–56, doi: 10.1016/S1342-937X(05)71083-2.

Watson EB (1982) Basalt contamination by continental crust: Some experiments and models. *Contributions to Mineralogy and Petrology* **80**, 73–87, doi: 10.1007/BF00376736.

Whitney DL and Evans BW (2010) Abbreviations for names of rock-forming minerals. *American Mineralogist* **95**, 185–87, doi: 10.2138/am.2010.3371.

Williams IS (1998) U-Th-Pb geochronology by ion microprobe. *Reviews in Economic Geology* **7**, 1–35.

Williams IS (2001) Response of detrital zircon and monazite, and their U–Pb isotopic systems, to regional metamorphism and host-rock partial melting, Cooma Complex, southeastern Australia. *Australian Journal of Earth Sciences* **48**, 557–80.

Winchester JA and Floyd PA (1977) Geochemical discrimination of different magma series and their differentiation products using immobile elements. *Chemical Geology* **20**, 325–43.

Zimmermann U, Niemeyer H and Meffre S (2010) Revealing the continental margin of Gondwana: The Ordovician arc of the Cordón de Lila (northern Chile). *International Journal of Earth Sciences* **99**, 39–56, doi: 10.1007/s00531-009-0483-8.